



HAL
open science

Characterization of a Human Point Mutation of VGLUT3 (p.A211V) in the Rodent Brain Suggests a Nonuniform Distribution of the Transporter in Synaptic Vesicles

Lauriane Ramet, Johannes Zimmermann, Tiphaine Bersot, Odile Poirel, Stéphanie de Gois, Katlin Silm, Diana Yae Sakae, Nina Mansouri-Guilani, Marie-Josée Bourque, Louis-Eric Trudeau, et al.

► To cite this version:

Lauriane Ramet, Johannes Zimmermann, Tiphaine Bersot, Odile Poirel, Stéphanie de Gois, et al.. Characterization of a Human Point Mutation of VGLUT3 (p.A211V) in the Rodent Brain Suggests a Nonuniform Distribution of the Transporter in Synaptic Vesicles. *Journal of Neuroscience*, 2017, 37 (15), pp.4181-4199. 10.1523/JNEUROSCI.0282-16.2017 . hal-01510648

HAL Id: hal-01510648

<https://hal.sorbonne-universite.fr/hal-01510648>

Submitted on 19 Apr 2017

HAL is a multi-disciplinary open access archive for the deposit and dissemination of scientific research documents, whether they are published or not. The documents may come from teaching and research institutions in France or abroad, or from public or private research centers.

L'archive ouverte pluridisciplinaire **HAL**, est destinée au dépôt et à la diffusion de documents scientifiques de niveau recherche, publiés ou non, émanant des établissements d'enseignement et de recherche français ou étrangers, des laboratoires publics ou privés.

1 Title:

2 **Characterization of a human point mutation of VGLUT3 (p.A211V) in the rodent brain**
3 **suggests a non-uniform distribution of the transporter in synaptic vesicles**

4
5 Abbreviated title:

6 VGLUT3 p.A211V mutation

7
8 Lauriane Ramet¹, Johannes Zimmermann², Tiphaine Bersot¹, Odile Poirel¹, Stéphanie De
9 Gois¹, Katlin Silm¹, Diana Yae Sakae¹, Nina Mansouri-Guilani¹, Marie-Josée Bourque³,
10 Louis-Eric Trudeau³, Nicolas Pietrancosta⁴, Stéphanie Daumas¹, Véronique Bernard¹,
11 Christian Rosenmund², Salah El Mestikawy^{1,5*}

12
13 ¹ Centre National de la Recherche Scientifique (CNRS) UMR 8246, Institut National de la
14 Santé et de la Recherche Médicale (INSERM), UMR-S 1130, Sorbonne Universités,
15 Université Pierre et Marie Curie (UPMC) Paris 06, Institut de Biologie Paris-Seine (IBPS),
16 UM119 Neuroscience Paris Seine, F-75005, Paris, France.

17 ² Neurocure NWFZ, Charite Universitaetsmedizin, 10117 Berlin, Germany

18 ³ Department of Pharmacology, Faculty of Medicine, GRSNC, Université de Montréal, QC,
19 Canada; Department of Neurosciences, Faculty of Medicine, GRSNC, Université de
20 Montréal, QC, Canada

21 ⁴ CNRS UMR-8601, Université Paris Descartes, CICB, Team Chemistry & Biology, Modeling
22 & Immunology for Therapy, CBMIT, 45 rue des Saint-Pères, 75006 Paris, France.

23 ⁵ Douglas Hospital Research Center, Department of Psychiatry, McGill University, 6875
24 boulevard Lasalle Verdun, QC, Canada

25
26 *Correspondence should be addressed to Salah El Mestikawy, Inserm U 1130, CNRS UMR
27 8246, Université Pierre et Marie Curie UM 119, 7 quai Saint Bernard, 75005, Paris, France.

28 E-mail: salah.el_mestikawy@upmc.fr

29

30 **Number of pages:** 47

31

32 **Number of:** Figures: 10

33 Tables: 3

34 3D models: 0

35

36 **Number of words for:** Abstract: 244

37 Statement: 114

38 Introduction: 652

39 Discussion: 2139 (1500)

40

41 **Conflict of Interests:** The authors declare no competing financial interests.

42

43 **Acknowledgements**

44 This research was supported by funds from the *Fondation pour la Recherche médicale*
45 (*Équipe* FRM DEQ20130326486), the *Agence Nationale pour la Recherche* (ANR), the
46 *Fédération pour la Recherche sur le Cerveau*, Labex (Bio-Psy Laboratory of Excellence),
47 INSERM, CNRS and UPMC.

48 LR received a PhD fellowship from the *Ministère de l'enseignement supérieur et de la*
49 *recherche* and from the *Fondation pour la Recherche médicale* (FDT20140930909).

50 We thank Géraldine Toutirais from the *Service de Microscopie Electronique of the Institut de*
51 *Biologie Paris-Seine* (Université Pierre et Marie Curie, Paris). We thank Valérie Nicolas from
52 the *Plateforme d'imagerie cellulaire of the Institut Paris Saclay d'Innovation Thérapeutique*
53 (UMS IPSIT Université Paris-Sud – US 31 INSERM – UMS 3679 CNRS, Châtenay-Malabry)
54 for assistance with STED microscopy. We thank Christoph Biesemann for the lentivirus
55 constructs, Stéphanie Pons and Martine Soudant as well as l'*École des Neurosciences de*
56 *Paris* (ENP) ("Network for Viral Transfer") for producing the lentiviruses.

57

58

59 **Abstract**

60

61 The atypical vesicular glutamate transporter type 3 (VGLUT3) is expressed by sub-
62 populations of neurons using acetylcholine, GABA or serotonin as neurotransmitters. In
63 addition, VGLUT3 is expressed in the inner hair cells of the auditory system. A mutation
64 (p.A211V) in the gene that encodes VGLUT3 is responsible for progressive deafness in two
65 unrelated families. In this study, we investigated the consequences of the p.A211V mutation
66 in cell cultures and in the central nervous system (CNS) of a mutant mouse. The mutation
67 substantially decreased VGLUT3 expression (-70%). We measured VGLUT3-p.A211V
68 activity by vesicular uptake in BON cells, electrophysiological recording of isolated neurons
69 and its ability to stimulate serotonergic accumulation in cortical synaptic vesicles. Despite a
70 marked loss of expression, the activity of the mutated isoform was only minimally altered.
71 Furthermore, mutant mice displayed none of the behavioral alterations that have previously
72 been reported in VGLUT3 knockout mice. Finally, we used stimulated emission depletion
73 microscopy (STED) to analyze how the mutation altered VGLUT3 distribution within the
74 terminals of mice expressing the mutated isoform. The mutation appeared to reduce the
75 expression of the VGLUT3 transporter by simultaneously decreasing the number of
76 VGLUT3-positive synaptic vesicles and the amount of VGLUT3 per synapses. These
77 observations suggested that VGLUT3 global activity is not linearly correlated with VGLUT3
78 expression. Furthermore, our data unraveled a non-uniform distribution of VGLUT3 in
79 synaptic vesicles. Identifying the mechanisms responsible for this complex vesicular sorting
80 will be critical to understand VGLUT's involvement in normal and pathological conditions.

81

82 Significance Statement

83

84 VGLUT3 is an atypical member of the vesicular glutamate transporter family. A point
85 mutation of VGLUT3 (VGLUT3-p.A211V) responsible for a progressive loss of hearing has
86 been identified in humans. We observed that this mutation dramatically reduces VGLUT3
87 expression in terminals (approximately 70%) without altering its function. Furthermore, using
88 stimulated emission depletion (STED) microscopy, we found that reducing the expression
89 levels of VGLUT3 diminished the number of VGLUT3-positive vesicles at synapses. These
90 unexpected findings challenge the vision of a uniform distribution of synaptic vesicles at
91 synapses. Therefore, the overall activity of VGLUT3 is not proportional to the level of
92 VGLUT3 expression. These data will be key in interpreting the role of VGLUTs in human
93 pathologies.

94

95 INTRODUCTION

96

97 Glutamate accumulation within synaptic vesicles (SVs) is facilitated by the vesicular
98 glutamate transporters VGLUT1, VGLUT2 and VGLUT3 (for review see (El Mestikawy et al.,
99 2011)). VGLUTs are crucial anatomical and functional markers of glutamatergic
100 transmission. The amount of glutamate that is packaged into SVs and the amount of
101 glutamate that is released are believed to be proportional to the density of VGLUT
102 expression (Daniels et al., 2004; Wilson et al., 2005; Daniels et al., 2006; Moechars et al.,
103 2006; Daniels et al., 2011). In addition to glutamate vesicular packaging, additional roles for
104 the VGLUTs have recently been revealed. For example, VGLUTs influence the mobility of
105 SVs in the axon and their stability in the synapse, as well as the intrinsic release probability
106 of glutamatergic vesicles (Weston et al., 2011; Siksou et al., 2013; Herman et al., 2014).

107 The VGLUTs are structurally and functionally similar but are anatomically segregated.
108 VGLUT1-2 are used by cortical and subcortical excitatory terminals, respectively (Bellocchio
109 et al., 2000; Takamori et al., 2000; Fremeau et al., 2001; Herzog et al., 2001; Takamori et al.,
110 2001; Varoqui et al., 2002). In contrast, VGLUT3 is localized in small populations of neurons
111 using neurotransmitters other than glutamate, such as cholinergic interneurons in the
112 striatum, subsets of GABAergic interneurons in the hippocampus and cortex and
113 serotonergic neurons in the dorsal and median raphe nuclei (Fremeau et al., 2002; Gras et
114 al., 2002; Schafer et al., 2002; Takamori et al., 2002; Herzog et al., 2004). At the cellular
115 level, VGLUTs are present in terminals. However, unlike VGLUT1 and VGLUT2, VGLUT3 is
116 also observed in somato-dendritic compartments (Herzog et al., 2004). VGLUT3 facilitates
117 vesicular accumulation and release of acetylcholine, serotonin and GABA via a mechanism
118 called “vesicular synergy” (Gras et al., 2008; Amilhon et al., 2010; Zander et al., 2010).
119 VGLUT3 confers on “non-glutamatergic” cells the ability to release glutamate (Varga et al.,
120 2009; Higley et al., 2011; Nelson et al., 2014).

121 Mice that no longer express VGLUT3 (VGLUT3^{-/-}) display hypersensitivity to pain, increased
122 anxiety and increased sensitivity to cocaine (Gras et al., 2008; Seal et al., 2009; Amilhon et

123 al., 2010; Peirs et al., 2015; Sakae et al., 2015). Interestingly, heterozygous mice display no
124 specific altered phenotype.

125 VGLUT3 is expressed by sensory inner hair cells in the auditory system. Therefore,
126 VGLUT3^{-/-} mice are profoundly deaf (Ruel et al., 2008; Seal et al., 2008). In humans, the
127 p.A211V mutation of the gene that encodes VGLUT3 (*Slc17a8*) is responsible for a type of
128 progressive deafness, DFNA25 (Ruel et al., 2008). This observation was the first evidence of
129 an association between human pathology and a VGLUT mutation.

130 The mutated alanine is part of a peptide sequence that is highly conserved among the
131 VGLUTs and their orthologs. The A211 alanine in human VGLUTs corresponds to position
132 224 in the mouse VGLUT3 sequence (A224). In this report, we generated a mutant mouse
133 carrying the p.A211V mutation (VGLUT3^{A224V/A224V}) and investigated its effects on the CNS.
134 The VGLUT3^{A224V/A224V} mice present the same progressive loss of hearing reported in
135 humans ((Ruel et al., 2008), Miot et al., manuscript in preparation).

136 In the CNS, we observed that the amount of mutated VGLUT3-p.A224V protein was
137 dramatically reduced in nerve endings (~70%). Moreover, VGLUT3-dependent vesicular
138 accumulation and synaptic release of glutamate were only minimally altered in
139 VGLUT3^{A224V/A224V} mice. Increased anxiety as well as increased basal or cocaine-induced
140 locomotor activity have been observed in VGLUT3^{-/-} mice. Despite substantial loss of
141 VGLUT3, VGLUT3^{A224V/A224V} mice displayed no such behavioral alterations. Therefore, the
142 molecular, cellular and behavioral functions of VGLUT3 are as efficiently fulfilled with 100%
143 or with 30% expression of the transporter. This observation suggests that VGLUT3 global
144 activity is not linearly correlated with the amounts of VGLUT3 present in terminals.

145 Finally, with stimulated emission depletion (STED) microscopy, we observed a decrease of
146 VGLUT3-p.A224V-positive vesicles in the terminals. Together, these observations establish
147 that the p.A211V mutation has complex effects on VGLUT3 expression and targeting.

148

149 **MATERIALS AND METHODS**

150

151 *Animals*

152 Animal care and experiments were conducted in accordance with the European
153 Communities Council Directive for the Care and the Use of Laboratory Animals (86/809/EEC)
154 and in compliance with the *Ministère de l'Agriculture et de la Forêt, Service Vétérinaire de la*
155 *Santé et de la Protection Animale* (authorization # 01482.01 from ethics committee Darwin
156 #5). All efforts were made to minimize the number of animals used in the course of the study
157 and to ensure their well-being. The animals were housed in a temperature-controlled room
158 (21± 2°C) with free access to water and food under a light/dark cycle of 12 h (light 7:30 -
159 19:30).

160

161 *Construction, genotyping and breeding of VGLUT3^{A224V/A224V} and VGLUT3^{A224V/-} mice*

162 The p.A211V mutation has been described in two unrelated human families (Ruel et al.,
163 2008). The alanine at position 211 of human VGLUT3 is part of a KWAPPLER motif and is
164 highly conserved in all three VGLUTs among different species (Ruel et al., 2008). In mouse
165 VGLUT1 and VGLUT3, this alanine is at positions 198 and 224, respectively (Fig. 1A). A
166 mouse line expressing the p.A224V mutation was generated at Phenomin - iCS (Phenomin-
167 Institut Clinique de la Souris-, Illkirch, France; <http://www.phenomin.fr/>) and was named
168 VGLUT3^{A224V/A224V}. A point mutation was introduced in exon 5 of the mouse *Slc17a8* gene: a
169 GCG (coding for an alanine) was exchanged for a GTG (coding for a valine) (Fig. 1B). Mice
170 were genotyped by PCR analysis of tail DNA with the following PCR primers: (p1) 5'-
171 CGGAGGGGAAGCCAGGAAAGGG-3' and (p2) 5'-
172 GACAGCTCAGTGAGCTGTAGACCCAG-3' for the WT and the mutated allele, yielding
173 bands of 219 and 306 bp, respectively (Fig. 1C).
174 Mice used in the study were aged 10 days to 12 months. They were obtained by crossing
175 heterozygous VGLUT3^{A224V/+} (C57BL/6N genetic background) or VGLUT3^{+/-} (VGLUT3^{-/-},
176 (Sakae et al., 2015)) mice with VGLUT3^{A224V/+} (C57BL/6N) mice (Table I). Breeding provided

177 mice expressing either: i) 2 copies of the VGLUT3 WT allele (VGLUT3^{+/+} or WT), ii) one copy
178 of mutated and one copy of VGLUT3 WT allele (VGLUT3^{A224V/+}), iii) 2 copies of mutated
179 alleles (VGLUT3^{A224V/A224V}) or iv) only one copy of mutated alleles (VGLUT3^{A224V/-}).

180 Male littermates were used for the behavioral analysis, and females or males were used for
181 the anatomical and biochemical experiments. The animals were randomly allocated to the
182 experimental groups. Whenever possible, investigators were blinded to the genotypes during
183 the experimental procedures. Animals were excluded from the experimental data analysis
184 only when their results were detected as outliers using Grubb's test (GraphPad Prism
185 software, La Jolla, CA USA).

186

187 *Behavioral experiments*

188 *Spontaneous locomotor activity:* Basal locomotor activity was assessed as previously
189 described (Gras et al., 2008). Mice were placed individually in activity boxes (20 x 15 x 25
190 cm), where their horizontal and vertical activities were measured by photocell beams located
191 across the long axis, 15 mm (horizontal activity) and 30 mm (vertical activity) above the floor.
192 Each box was connected by an interface to a computer (Imetronic). Spontaneous locomotor
193 activity was measured in 15 min intervals over five hours between 18:30 and 23:30 p.m.

194 *Open field (OF):* The open field test was performed in a white Perspex arena (43 x 43 x 26
195 cm) located in a 10 lux illuminated room, as previously reported (Amilhon et al., 2010). The
196 virtual central compartment square represented 1/3 of the total arena. Mice were introduced
197 into the central area and allowed to freely explore the open field for 360 sec. The durations,
198 frequencies and time courses of various behaviors (exploration, walking, rearing, stretching
199 and grooming) were measured in different regions of the open field (central vs periphery
200 zone). The time and number of entries in the center of the open field were evaluated as an
201 index of an anxiety-related response.

202 *Elevated plus maze (EPM):* EPM was used to measure unconditioned anxiety-like behavior
203 (Amilhon et al., 2010). The EPM, which consisted of two open arms, two enclosed arms and
204 a central platform elevated 38.5 cm above the ground, was placed into 10 lux ambient light.

205 After being allowed one hour of habituation in the testing room, the animals were placed in
206 the central area, facing one of the closed arms, and were tested for 360 sec. The total time
207 spent in each compartment (open vs closed arms) was recorded by video tracking
208 (Viewpoint).

209 *Cocaine-induced locomotor activity:* Cocaine-induced locomotor activity was measured in a
210 cyclotron, which consisted of a circular corridor with four infrared beams placed at 90° angles
211 (Imetronic). Activity was counted as the consecutive interruption of two adjacent infrared
212 beams (1/4 of a tour). To assess acute cocaine-induced locomotion, the animals were i)
213 placed in the cyclotron for four hours for habituation, ii) injected with saline (NaCl 0.9%) and
214 placed back in the cyclotron for 60 min and iii) injected with cocaine (10 mg/kg,
215 intraperitoneal (i.p)). Locomotion was recorded for 95 min following cocaine injection.

216

217 *Neuronal microculture and electrophysiological recording of autapses*

218 Hippocampi were harvested at postnatal day 0 (P0) to P1 from VGLUT1^{-/-} mice of either sex
219 (Wojcik et al., 2004). Neurons were plated on island cultures at a density of 2000-3000
220 neurons per 35 mm dish. Recordings were performed from 14 to 18 DIV. VGLUT1^{-/-} autaptic
221 neurons were infected with either VGLUT3 or VGLUT3-p.A211V lentiviral vectors
222 (respectively: 10 and 40 ng p24 per well). In order to normalize expression levels and to
223 compare electrophysiological activity of the 2 isoforms, five times more VGLUT3-p.A211V
224 than WT expressing viral particles were used to rescue VGLUT1^{-/-} hippocampal neurons.

225 The standard extracellular solution contained the following (in mM): 140 NaCl, 2.4 KCl, 10
226 HEPES, 10 glucose, 4 MgCl₂, and 2 CaCl₂, pH 7.3. The internal solution contained the
227 following (in mM): 135 KCl, 18 HEPES, 1 EGTA, 4.6 MgCl₂, 4 ATP, 0.3 GTP, 15 creatine
228 phosphate, and 20 U/ml phosphocreatine kinase. Excitatory postsynaptic currents (EPSCs)
229 were evoked by 2 ms of depolarization at 0 mV, resulting in an unclamped action potential.
230 Readily releasable vesicle pool (RRP) size was assessed by pulsed (5 s) application of
231 hypertonic sucrose solution (500 mM sucrose added to extracellular solution) and by
232 integrating the transient inward current component. Vesicular release probability was

233 computed by dividing the EPSC charge by the RRP charge. Current traces were analyzed
 234 using Axograph X (Axograph), Excel (Microsoft) and Prism (GraphPad). The mEPSCs were
 235 detected with a template function (Axograph; template: rise, 0.5 ms; decay, 3 ms; criteria
 236 range: rise, 0.15-1.5 m; decay, 0.5-5 ms).

237

238 *In situ hybridization labeling of VGLUT3 mRNA*

239 Regional *in situ* hybridization was performed as previously described (Gras et al., 2008;
 240 Amilhon et al., 2010; Vigneault et al., 2015). Mouse brains were rapidly dissected and frozen
 241 in isopentane at -30°C. Coronal brain sections (12 μ m) were cut with a cryostat (Leica
 242 Biosystems) at -20°C, thaw-mounted on glass slides, fixed in 4% formaldehyde, washed with
 243 PBS, dehydrated in 50% and 70% ethanol and air-dried. The sections were incubated with a
 244 mixture of 9 antisense oligonucleotides specific for mouse VGLUT3 (5'-
 245 TCAGAAGCTGTCATCCTCTCTCAACTCCAG-3', 5'-
 246 GGCATCTTCCTCTTCATTGGTCCCATCGAT-3', 5'-
 247 CCCTTCTCCTCTCGATCCAGAATCAACAAA-3', 5'-
 248 ACTGCGCTTGCCCTGGAGGAACACTTGAAA-3', 5'-
 249 GCCGTAATGCACCCTCGCCGCAGAAGGGATAAAC-3', 5'-
 250 GGGCAGCCAAGCTCAGAATGAGCACAGCCTGTATCC-3', 5'-
 251 AGTCACAGATGTACCGCTTGGGGATGCCGCAGCAG-3', 5'-
 252 AGCCAGTTGTCCTCCGATGGGCACCACGATTGTC-3' and 5'-
 253 CCACAATGGCCACTCCAAGGTTGCACCGAATCCC-3'). These oligonucleotides were
 254 labeled with [³⁵S]-dATP (Perkin Elmer) to a specific activity of 5 x 10⁸ dpm/ μ g using terminal
 255 deoxynucleotidyl transferase (Promega). Sections were incubated for 18 h at 42°C, washed
 256 and exposed to a BAS-SR Fujifilm Imaging Plate for seven days. The plates were scanned
 257 with a Fuji Bioimaging Analyzer BAS-5000. Densitometry measurements were performed
 258 with MCIDTM analysis software. Densitometric analysis of 4-6 sections for each region was
 259 averaged per mouse (8 mice per genotype).

260

261 *Immunoautoradiographic labeling of VGLUT3*

262 Immunoautoradiography experiments were performed on fresh frozen mouse brain sections
263 (12 μm) as previously described (Amilhon et al., 2010; Vigneault et al., 2015). Brain slices
264 were incubated with VGLUT3 rabbit polyclonal antiserum (1:20,000, Synaptic Systems) and
265 then with anti-rabbit [^{125}I]-IgG (Perkin Elmer). The sections were then washed in PBS, rapidly
266 rinsed in water, dried and exposed to X-ray films (Biomax MR, Kodak) for five days. Standard
267 radioactive microscaleres were exposed to each film to ensure that labeling densities were in
268 the linear range. Densitometry measurements were performed with MCIDTM analysis
269 software on 4-6 sections for each region per mouse (8 mice per genotype).

270

271 *Immunofluorescence*

272 Immunofluorescence experiments were performed on BON cells, hippocampal primary
273 neurons and brain slices, as previously described (Herzog et al., 2001; Gras et al., 2002;
274 Herzog et al., 2011). Cells or brain sections were incubated with anti-human VGLUT3 rabbit
275 polyclonal antiserum (1:1000, (Vigneault et al., 2015))(Gras et al., 2002), anti-rodent
276 VGLUT3 rabbit polyclonal antiserum (1:2000, Synaptic Systems), anti-rodent VGLUT1 rabbit
277 polyclonal antiserum (1:2000, (Herzog et al., 2001)), anti-rodent MAP2 mouse monoclonal
278 antiserum (1:1000, Sigma), anti-rodent bassoon mouse monoclonal antiserum (1:2000,
279 Abcam) or PSD95 mouse monoclonal antiserum (1:2000, Abcam). Immunolabeling was
280 detected with anti-rabbit or anti-mouse secondary antisera coupled to Alexa Fluor 555 or
281 Alexa Fluor 488 (1:2000, Invitrogen). Nuclei were labeled using DAPI (1:5000, Sigma). The
282 cells and sections were observed with a fluorescence microscope equipped with an Apotome
283 module (Zeiss, Axiovert 200 M) or a confocal Laser Scanning Microscope (Leica TCS SP5,
284 Leica Microsystems). Fluorescence intensity in the synaptic boutons of hippocampal
285 neuronal cultures was quantified using the MacBiophotonics plugins package for ImageJ
286 software. In the brain slices, semi-quantification of VGLUT3 in the soma and terminals was
287 performed with ImageJ software (Macbiophotonics plugins). The contour of neuronal soma or
288 brain areas containing terminals were delineated manually and the integrated intensity within

289 these region of interest (ROI) were measured using the ROI manager of the ImageJ
290 software.

291

292 *Electron microscopy immunogold detection of VGLUT3*

293 Electron microscopy experiments were performed on WT and VGLUT3^{A224V/A224V} mice, as
294 previously described (Bernard et al., 1999; Herzog et al., 2001). Briefly, the animals were
295 deeply anesthetized and perfused transcardially with a mixture of 2% paraformaldehyde in
296 0.1 M phosphate buffer (pH 7.4) and 0.2% glutaraldehyde. Their brains were dissected, fixed
297 overnight in 2% paraformaldehyde and stored in PBS until use. Sections (70 μ m) from the
298 midbrain, including the striatum, were cut on a vibrating microtome (Leica Biosystems,
299 VT1000S). Sections were successively incubated in anti-rodent VGLUT3 rabbit polyclonal
300 antiserum (1:2000, Synaptic System), in goat anti-rabbit coupled to biotin (Vector
301 laboratories) and in streptavidin coupled to gold particles (0.8 nm in diameter; Nanoprobes;
302 1:100 in PBS/BSA-C). The signal of the gold immunoparticles was increased using a silver
303 enhancement kit (HQ silver; Nanoprobes) for 2 min at RT in the dark. Finally, after treatment
304 with 1% osmium, dehydration and embedding in resin, ultrathin sections were cut, stained
305 with lead citrate and examined in a transmission electron microscope (EM 912 OMEGA,
306 ZEISS) equipped with a LaB6 filament at 80kV. Images were captured with a digital camera
307 (SS-CCD, 2kx2k, Veleta).

308

309 *VGLUT3 immuno-detection by STED microscopy*

310 STED microscopy experiments were performed on WT, VGLUT3^{A224V/+}, VGLUT3^{A224V/A224V},
311 VGLUT3^{A224V/-} and VGLUT3^{-/-} mice. Briefly, the animals were deeply anesthetized and
312 perfused transcardially with paraformaldehyde (2%). Their brains were dissected, fixed
313 overnight in 2% paraformaldehyde and stored in PBS until use. Sections (70 μ m) from the
314 midbrain, including the striatum, were cut on a vibrating microtome (Leica, VT1000S).
315 VGLUT3 was detected in axonal varicosities in the mouse caudate putamen. To ensure that
316 VGLUT3 was detected in varicosities, synaptophysin I, a synaptic vesicular protein, was co-

317 detected with VGLUT3. Sections were successively incubated in a mixture of anti-rodent
318 VGLUT3 rabbit polyclonal antiserum (1:2000, Synaptic System) and anti-synaptophysin I
319 mouse antiserum (1:2000, Synaptic System), in anti-mouse biotinylated secondary antibody
320 (1:100, Vector Laboratories), and in a mixture of Streptavidin (1:100, BD Horizon™ V500,
321 BD Biosciences) and Oregon Green 488 goat anti-rabbit IgG (Thermo Fisher Scientific) and
322 mounted in ProLong Gold (Thermo Fisher Scientific).

323 Sections were observed using a SP8 gated-STED microscope (Leica Microsystems)
324 equipped with a 592 nm depletion laser. BD Horizon™ V500 and Oregon Green 488 were
325 excited at 470 nm and 514 nm, respectively. All acquisitions were performed using the same
326 excitation laser power (50%). Alternatively, we compared the effect of increased laser power
327 on the number of spots (50, 75, 100%). Images were submitted to deconvolution (Huygens
328 software, Scientific Volume Imaging), which permits the recovery of objects that are
329 degraded by blurring and noise. Finally, the images were analyzed using ImageJ and Adobe
330 Photoshop. The number of VGLUT3-positive puncta per varicosity surface was quantified in
331 each genotype (80, 76, 76, 90, 105 varicosities per animals were quantified in 6 WT, 6
332 VGLUT3^{A224V/+}, 6 VGLUT3^{A224V/A224V}, 6 VGLUT3^{A224V/-} and 5 VGLUT3^{-/-} mice, respectively).

333

334 *Fluorescence recovery after photobleaching (FRAP)*

335 FRAP experiments were performed to compare the mobility of VGLUT3-p.A211V with that of
336 wild-type VGLUT3 at synapses. Primary culture of hippocampal neurons (as described
337 below) were infected 48 h after plating with either VGLUT3 or VGLUT3-p.A211V lentiviral
338 vectors (respectively: 10 and 40 ng p24 per well). In order to normalize expression levels of
339 the 2 isoforms, five times more VGLUT3-p.A211V than WT expressing viral particles were
340 used to infect hippocampal primary neurons. Experiments were performed as previously
341 described (Herzog et al., 2011) using a SP5 Laser Scanning Microscope (Leica) with a
342 63X/1.32 numerical aperture oil-immersion objective and a thermal incubator set to 37°C
343 surrounding the setup (Leica Microsystems). The pinhole was opened to 2.5 Airy units to
344 enhance signal detection. A bleaching protocol was used to prevent spontaneous recovery of

345 venus fluorescence, as previously reported (McAnaney et al., 2005). Fluorescence recovery
346 was monitored every 30 s during the first 5 min and then every 5 min for the next 70 min for
347 FRAP and every 5 s for 10 min for Fast FRAP. The entire FRAP and Fast FRAP procedures
348 were automated using SP5 live data mode software. Image processing was automated using
349 ImageJ macro commands. Integrated fluorescence intensities were extracted from six
350 bleached and eight control boutons, as well as one background area. The background signal
351 was subtracted.

352

353 *BON cell culture and transfection*

354 Human carcinoid BON cells were maintained in 1:1 DMEM/F-12 medium supplemented with
355 10% fetal bovine serum (PAA Laboratories, GE Healthcare Life Sciences), 100 units/ml
356 penicillin and 100 μ g/ml streptomycin (Life Technologies) at 37°C in a humidified 5% CO₂
357 incubator as previously described (Herzog et al., 2001; Gras et al., 2002). BON cells were
358 transfected using Lipofectamine 2000 (Thermo Fisher Scientific) according to the
359 manufacturer's instructions with the expression vector pcDNA3 (Invitrogen) containing the
360 sequence coding for human VGLUT3 or VGLUT3-p.A211V coupled to green fluorescent
361 protein (GFP) reporter (pcDNA3-VGLUT3-IRES-GFP or -VGLUT3-p.A211V-IRES-GFP).
362 Stable clones were selected using G418 antibiotics (Merck, Millipore), and flow cytometry
363 was used to select GFP- and VGLUT3-positive cells. Stable clones expressing VGLUT3 or
364 VGLUT3-p.A211V were maintained in culture medium containing G418 (0.6 mg/ml).

365

366 *Hippocampal neuronal culture*

367 For immunofluorescence experiments, hippocampal cell cultures were prepared from
368 newborn P0-P2 (P0 being the day of birth) C57BL/6 pups of either sex as previously
369 described (Fasano et al., 2008). After seven days in culture, neurons were transfected with
370 linearized plasmid pcDNA3-VGLUT3-IRES-GFP or pcDNA3-VGLUT3-p.A211V-IRES-GFP
371 with lipofectamine 2000 (Thermo Fisher Scientific, 1 μ g of DNA for 1 μ l of lipofectamine). At 9
372 day *in vitro* (DIV), neurons were fixed and immunofluorescence experiments were performed.

373 For Fluorescence recovery after photobleaching (FRAP) experiments, hippocampal cell
374 cultures were prepared as previously described (Siksou et al., 2013). After 2 days in culture,
375 neurons were infected with lentiviral vectors containing either VGLUT3-venus or VGLUT3-
376 p.A211V-venus inserts under the control of the synapsin promoter (respectively: 10 and 40
377 ng p24 per well). Viral particles expressing VGLUT3-venus or VGLUT3-p.A211V-venus were
378 diluted 1:1000 in neurobasal medium (Life Technologies) containing Glutamax (Thermo
379 Fisher Scientific), B27 and penicillin/streptomycin (Sigma-Aldrich). The diluted virus solutions
380 (50 μ l at and 300 μ l for VGLUT3-venus and VGLUT3-p.A211V-venus expressing lentivirus,
381 respectively) were incubated for 15 days with the primary neuronal cultures. FRAP imaging
382 of live dissociated neuron cultures was performed at 17 DIV.

383

384 *Mutagenesis and construction of VGLUT3-p.A211V and VGLUT1-p.A198V*

385 To introduce a point mutation in the WT alleles, we used the QuikChange II XL Site-Directed
386 Mutagenesis Kit (Stratagene) and a set of complementary primers as previously described
387 (De Gois et al., 2015). All clones were sequenced in both directions, and the plasmids were
388 purified using a Plasmid Maxi Kit (Qiagen) before use.

389

390 *Vesicular glutamate uptake assay with vesicles from stable BON clones*

391 Synaptic vesicle preparations from the BON cells and [³H]L-glutamate uptake assays were
392 performed as previously described (Herzog et al., 2001; Gras et al., 2002). Transport activity
393 was triggered by the addition of 20 μ l of vesicles (200 μ g of protein) to 180 μ l of uptake buffer
394 containing ATP (2 mM, Sigma-Aldrich), L-glutamate (40 μ M pH 7.4, Sigma-Aldrich) and
395 [³H]L-glutamate (6 μ Ci, Perkin Elmer) with or without carbonyl cyanide m-
396 chlorophenylhydrazone (CCCP, 50 μ M, Sigma-Aldrich). After 10 min at 37°C, the uptake
397 assays were terminated by dilution with 3 ml of ice-cold 0.15 M KCl, rapid filtration through a
398 0.45 μ m pore size membrane filter (MF, Millipore), and three washes with 3 ml of ice-cold
399 0.15 M KCl. The radioactivity retained on the filters was measured by scintillation counting.

400 Each uptake measurement was performed in triplicate. All experiments were performed
401 independently three times on three independent BON-VGLUT3 clones.

402
403 *Vesicular [³H]5-HT uptake assay in mouse brain synaptic vesicles*

404 Synaptic vesicle isolation from mouse cortex and uptake assays of [³H]5-HT were performed
405 as previously described (Amilhon et al., 2010). Transport reactions were initiated by adding
406 10 μ l of cortical synaptic vesicles (25 μ g of protein) to 90 μ l of uptake buffer containing ATP
407 (2 mM, Sigma-Aldrich) and [³H]5-HT (0.55 μ Ci, 50 nM, Perkin Elmer) with or without 2 μ M
408 reserpine (Sigma-Aldrich) or L-glutamate (10 mM, Sigma-Aldrich). After 10 min at 37°C,
409 vesicular uptake was stopped by dilution in 3 ml of ice-cold 0.15 M KCl, rapid filtration
410 through mixed cellulose esters filters (MF, Millipore), and three washes with 3 ml of ice-cold
411 0.15 M KCL. Radioactivity retained on the filters was measured by scintillation counting.
412 Each determination was performed in triplicate and independent experiments were
413 performed seven times using different synaptic vesicle preparations.

414
415 *Western blotting*

416 Western blot experiments were conducted on BON cell extracts or on homogenates from
417 different brain regions (cortex, striatum, hippocampus), as previously described (Gras et al.,
418 2008; Vigneault et al., 2015). Nitrocellulose membranes (0.4 μ m pore size, Invitrogen) were
419 incubated overnight with anti-human VGLUT3 rabbit polyclonal antiserum (1:1000, (Vigneault
420 et al., 2015)), anti-rodent VGLUT3 rabbit polyclonal antiserum (1:2000, Synaptic Systems) or
421 anti-rodent VGLUT1 rabbit polyclonal antiserum (1:5000, (Herzog et al., 2001)) and then with
422 IRDye 800 conjugated secondary antibodies (1:5000, Invitrogen). Alpha-tubulin was used as
423 loading control (mouse monoclonal antiserum, 1:20,000, Sigma-Aldrich) detected with IRDye
424 700 conjugated secondary antibodies (1:5000, Invitrogen). The membranes were scanned
425 using an Odyssey infrared imaging system (LI-COR). Integrated intensity was measured for
426 each band and averaged for 5-7 samples.

427

428 *Quantitative reverse transcription-PCR analysis*

429 The expression of VGLUT3 transcript in stable BON cells was estimated by quantitative
430 reverse transcription PCR (RT-PCR), as previously described (Gras et al., 2002). Nucleic
431 acids were extracted from 65×10^4 BON cells (RNAeasy Mini Kit, Qiagen). Reverse
432 transcription was performed with a SuperScript® Reverse Transcriptase Kit (Life
433 Technologies) using 2 μ g of nucleic-acid extract. cDNA amplification was performed with
434 Taq™ DNA polymerase (Sigma-Aldrich), and the following primers: 5'-
435 ACTCTGAACATGTTTATTCCC-3' and 5'-CTTAGACTAACCACGTTGGC-3' (3 min. at 94°C
436 followed by 30 sec. at 94°C, 30 sec. at 55°C and 40 sec. at 72°C for 40 cycles). The RT-PCR
437 products were separated on 1% agarose gel and viewed under UV light. Intensity
438 quantification was performed with ImageJ software (Macbiophotonics plugins).

439

440 *Homology modeling of VGLUT3*

441 A putative 3D structure of VGLUT3 was established based on the X-ray crystal structure of
442 the glycerol-3-phosphate transporter (GlpT) from *Escherichia coli*, which is a distant ortholog
443 of vesicular glutamate carriers (Almqvist et al., 2007). Secondary structures were predicted
444 using the membrane protein topology prediction method TransMembrane prediction using
445 Hidden Markov Models (TMHMM) and a Hidden Markov Model for Topology Prediction
446 (HMMTOP) (Krogh et al., 2001; Tusnady and Simon, 2001). Sequence alignments were
447 generated between human VGLUT3 (SWISS-PROT accession n°: Q8NDX2) and GlpT
448 (P08194) using Clustal W (Thompson et al., 1994). Alignments were manually refined to
449 avoid gaps in predicted (human VGLUT) and known (GlpT) secondary structure elements.
450 VGLUT3 3D models were built from these alignments and from the crystallographic atomic
451 coordinates of GlpT (PDB ID: 1PW4) using the automated comparative modeling tool
452 MODELER 9.0 (Discovery Studio 4.1, Accelrys Software Inc.). A three-dimensional model of
453 the VGLUT3-p.A211V mutant was generated using a Build mutant protocol (Feyfant et al.,
454 2007). The mutant model was minimized using the Adopted Basis Newton-Raphson (NR)
455 algorithm, with a maximum step of 500 and a “generalized Born with Implicit Membrane

456 (GBIM)" as an implicit solvent model. A 1-palmitoyl-2-oleoyl-phosphatidylcholine (POPC)
457 membrane of 100 x 80 angstroms was added using software from Visual Molecular Dynamic
458 (VMD 1.9.2, <http://www.ks.uiuc.edu/Research/vmd/vmd-1.9.2/>). Proteins were solvated, and
459 ions were added using the solvation and ionization package from VMD1.9.2. The structure
460 was minimized using a Adopted Basis Newton-Raphson (NR) algorithm, with a maximum
461 step of 500 and an implicit solvent model. The system was then equilibrated using a short
462 Nanoscale Molecular Dynamic software program (NAMD) of 1 ns.

463

464 *Statistics*

465 All statistical comparisons were performed with Prism 5 (GraphPad software Inc.). Each
466 statistical test was appropriately chosen for the relevant experimental design. To compare
467 two groups, a non-parametric Mann-Whitney U test was performed. One-way ANOVA,
468 Kruskal-Wallis test or repeated-measures ANOVA was used for multiple group comparisons.
469 All results are expressed as the mean \pm SEM. Differences were considered significant at $p <$
470 0.05.

471

472 **RESULTS**

473

474 **The VGLUT3-p.A211V mutation reduces the expression level of VGLUT3 *in vitro***

475 To compare the expression of native VGLUT3 and VGLUT3-p.A211V, both alleles were
476 expressed in cultures of stably transfected BON cells or hippocampal neurons. The
477 transcripts coding for both isoforms were expressed at similar levels in BON cells when
478 detected by RT-PCR (Fig. 2A; Mann-Whitney U test, $p > 0.05$, $n = 6$). In contrast, VGLUT3-
479 p.A211V protein levels were markedly reduced relative to the WT isoform when measured by
480 western blotting in BON cells (Fig. 2B; -64%, Mann-Whitney U test, $p = 0.0079$, $n = 5$) or in
481 hippocampal neuronal cultures (Fig. 2C; -66%, Mann-Whitney U test, $p = 0.028$, $n = 4$). This
482 decrease was also confirmed by immunofluorescence detection of VGLUT3 and VGLUT3-
483 p.A211V in BON cells (Fig. 2D; G, H; -79%, Mann-Whitney U test, $p = 0.028$, $n = 4$) or in
484 hippocampal neuronal cultures (Fig. 2E, I, J; -86%, Mann-Whitney U test, $p = 0.008$, $n = 5$).
485 The same point mutation was then introduced into the coding sequence of VGLUT1
486 (VGLUT1-p.A198V). Interestingly, VGLUT1-p.A198V expression was dramatically reduced in
487 BON cells (Fig. 2F, K, L; -90%, Mann-Whitney U test, $p = 0.005$, $n = 6$). Therefore,
488 exchanging the alanine of the KWAPPLER motif for a valine was sufficient to markedly
489 reduce the expression of vesicular glutamate transporters.

490 We then assessed whether VGLUT3-p.A211V was expressed in synaptic boutons in
491 neuronal hippocampal cultures. Both VGLUT3 and VGLUT3-p.A211V were expressed in
492 punctiform structures apposed to MAP2-positive dendritic processes (Fig. 2M and N). These
493 VGLUT3- and VGLUT3-p.A211V-positive puncta co-localized with presynaptic markers, such
494 as bassoon, and were apposed to PSD95-positive elements (Fig. 2O-R). Thus, the p.A211V
495 mutation does not qualitatively alter the targeting of VGLUT3 to synaptic boutons.

496

497 Glutamate vesicular uptake and release are minimally altered by the p.A211V mutation

498 We then wondered whether p.A211V altered the 3D structure of VGLUT3. Theoretical
499 models (Fig. 3A-H) were obtained using the crystal structure of the Glycerol-3-Phosphate
500 Transporter (GlpT) from *E. coli* (PDB ID: 1PW4, 19% identity, 39% similarity with VGLUT3)
501 as a template (Almqvist et al., 2007). As shown in Fig. 3, in these putative 3D models,
502 alanine 211 is strategically located on a small cytoplasmic loop (cytoplasmic loop 4, CL4)
503 and at the top of the transporter pore. Switching a valine for an alanine in this position only
504 minimally modified the 3D structure of the loop. In particular, in the WT isoform, A211
505 interacted with the N-terminal domain through cysteine 67 hydrophobic binding (Fig. 3C, D),
506 as well as with leucine 214 in CL4. These interactions were potentially altered with the
507 p.A211V mutation (Fig. 3G, H). Both WT and mutant isoforms conserved a short distance
508 interaction pattern with CL4 (K209; W210; P212; P213; L214 and E215). However in the N-
509 terminal domain of the mutant, the interaction of A211 with C67 was abolished. In parallel,
510 A211 from WT isoform interacted with T289 of the Cytoplasmic loop 6. This interaction was
511 lost in the VGLUT3 p.A211V mutated isoform but was partially compensated by interactions
512 with residues of CL6: H276 and I287 (Fig. 3H).

513 The putative 3D model suggests also that the alanine residue of the WT and the valine
514 residue of VGLUT3-p.A211V faced the pore and hence could affect the entry of glutamate
515 into the lumen of synaptic vesicles. Therefore, [³H]L-glutamate accumulation was measured
516 in vesicular fractions from BON cells stably expressing VGLUT3 or VGLUT3-p.A211V. A
517 small but non-significant reduction in vesicular glutamate uptake was observed with the
518 VGLUT3-p.A211V isoform (Fig. 3I, Mann-Whitney U test, $p > 0.05$, $n = 10$). Hence, despite a
519 60-80% reduction in expression, the mutated VGLUT3 appeared to be as efficient as the WT
520 allele at translocating glutamate into vesicles.

521 The capacity for glutamate release from neurons expressing the VGLUT3-p.A211V isoform
522 was then evaluated by electrophysiological recordings. Autaptic hippocampal cultured
523 neurons obtained from newborn VGLUT1^{-/-} mice were rescued by lentiviral-driven
524 expression of either VGLUT3 (WT, black bars) or VGLUT3-p.A211V (red bars). Uninfected

525 neurons are shown with green bars. In these experiments, in order to determine the intrinsic
526 properties of the VGLUT3-p.A211V isoform, expression levels of the mutant were purposely
527 raised to equal WT. After two weeks in culture, synaptic responses were evoked by 2 ms
528 depolarization of the cell at 0 mV. This resulted in an unclamped action potential and release
529 of glutamate, which in turn generated EPSCs. The mean normalized EPSC peak amplitude
530 was not different between the WT (n = 72) and the VGLUT3-p.A211V (n = 73) neurons (Fig.
531 3J). This was in contrast to the EPSC responses from VGLUT1^{-/-} neurons, which showed a
532 severe reduction in synaptic response, demonstrating that the WT and the VGLUT3-p.A211V
533 mutant rescued responses equally. We, next determined the readily releasable pool (RRP)
534 size of VGLUT3, VGLUT3-p.A211V and VGLUT1^{-/-} neurons by applying hypertonic sucrose
535 (500 mM for 5 s; (Rosenmund and Stevens, 1996)). The charge in VGLUT1^{-/-} neurons was
536 reduced by 80%, as expected (Fig. 3K, n = 73, p < 0.01, (Wojcik et al., 2004)). VGLUT3 and
537 VGLUT3-p.A211V neurons had a similar RRP charge (Fig. 3K). The expression levels of WT
538 and VGLUT3-p.A211V as determined by immunofluorescence were not different (Fig. 3L).
539 Moreover, the facilitation of responses that were evoked in pairs of action potential
540 stimulation (25 ms interval, Fig. 3M) and the vesicular release probability were not different
541 between VGLUT3 (n = 72) and VGLUT3-p.A211V (n = 73) neurons (Fig. 3M). The release
542 probability in the VGLUT1^{-/-} neurons was reduced, as expected (Wojcik et al., 2004; Herman
543 et al., 2014).

544 Analysis of spontaneous release activity (trace sample in Fig. 3O) demonstrated that mean
545 mEPSC amplitude was slightly reduced in VGLUT3-p.A211V neurons compared with WT
546 neurons (Fig. 3P and Q; WT, n = 62; VGLUT3-p.A211V, n = 67; p < 0.005). The mean
547 frequency of mEPSCs was significantly different among all three groups (Fig. 3R). In
548 VGLUT1^{-/-} neurons, mEPSC frequency was reduced by 80% (Fig. 3R; 1,8 Hz, n = 51, p <
549 0.0005), a finding consistent with the reduced RRP size (Fig. 3K) and the results of a
550 previous publication (Wojcik et al., 2004). In VGLUT3-p.A211V expressing hippocampal
551 isolated neurons, mEPSC frequency was reduced by almost 30% (Fig. 3R; WT, 8,5 Hz, n =
552 72; VGLUT3-p.A211V, 6 Hz, n = 77, p < 0.005). The mEPSC charge was also slightly

553 decreased in VGLUT3-p.A211V neurons compared with WT neurons (Fig. 3S; WT, n = 62;
554 VGLUT3-p.A211V, n = 67; $p < 0.005$). Together, the results suggested that the p.A211V
555 mutation does not alter the quantity of glutamate release, the RRP size or the release
556 probability. In contrast, small reduction in spontaneous release activity was observed.

557

558 **The expression of VGLUT3-p.A224V is dramatically reduced in the terminals of the** 559 **mouse CNS**

560 The p.A211V mutation is responsible for DFNA25 progressive deafness (Ruel et al., 2008).
561 To gain insight into the underlying mechanisms, we used newly generated mutant mice, in
562 which the corresponding amino acid was mutated in the VGLUT3 mouse genome
563 (VGLUT3^{A224V/A224V}, Fig. 1). The expression levels of VGLUT3 mRNA and protein were
564 measured by *in situ* hybridization, immunautoradiography and western blotting at different
565 ages (P10, 3, 6 and 12 months) in WT, heterozygous and homozygous mice (Fig. 4).

566 As shown in Fig. 4, the levels of VGLUT3 transcript were unaltered in the striatum,
567 hippocampus and raphe area at all ages assessed. In contrast protein levels were markedly
568 altered at various ages in the striatum, hippocampus and raphe of VGLUT3^{A224V/A224V} mice
569 (Fig. 4 and Table II). In the striatum of VGLUT3^{A224V/A224V} mice, the level of the mutant
570 protein, as measured by immunautoradiography, was reduced by 76 to 85% compared with
571 that in WT mice at all ages (Fig. 4A-J and Table II; Mann Whitney U test for P10 and 12
572 months; Kruskal-Wallis test for 3 and 6 months; * $p < 0.05$, ** $p < 0.01$, *** $p < 0.001$). A
573 similar decrease in protein levels was observed in the hippocampus, as well as the raphe
574 nuclei, with 69-76% and 50-74% reductions measured in the respective tissues at the same
575 time points. Hence, the mean decrease across age and brain areas in VGLUT3^{A224V/A224V}
576 mice was 70.3% (SEM \pm 2.7, n = 12). Reduced VGLUT3-p.A224V levels were also
577 measured in mice expressing only one copy of the mutated gene and one copy of the WT
578 gene (3-and 6-month old heterozygous VGLUT3^{A224V/+} mice, Fig. 4 and Table II). In
579 heterozygous mice, the mean decrease was 34% (SEM \pm 4.1, n = 8). These results were
580 further confirmed by western blotting experiments performed in the cortex, striatum and

581 hippocampus in 3-month-old VGLUT3^{A224V/+} and VGLUT3^{A224V/A224V} mice (Fig. 4K-L and Table
582 II; Kruskal-Wallis test, * $p < 0.05$, ** $p < 0.01$, *** $p < 0.001$). In summary, VGLUT3
583 expression was globally reduced by 70% in the brains of VGLUT3^{A224V/A224V} mice of all ages.
584 To obtain mice with only one copy of the VGLUT3-p.A224V isoform, we crossed
585 heterozygous VGLUT3^{+/-} mice with heterozygous VGLUT3^{A224V/+} mice. As shown in Fig. 4E-
586 F, the decrease in VGLUT3 expression was more pronounced in VGLUT3^{A224V/-} than in
587 VGLUT3^{A224V/A224V} mice. In the striatum of 3-month-old VGLUT3^{A224V/-} mice, VGLUT3
588 expression was reduced by 84% (Mann-Whitney U test, $p = 0.012$ relative to WT, $n = 8$).
589 Moreover, 88% of the protein was lost in the hippocampus (Mann-Whitney U test, $p = 0.012$
590 relative to WT, $n = 8$) and 71% was lost in the raphe nuclei (Mann-Whitney U test, $p = 0.028$
591 relative to WT, $n = 4$). Therefore, mice with one copy of the VGLUT3-p.A224V isoform
592 demonstrate a larger decrease in VGLUT3 expression than mice expressing 2 mutant
593 copies.

594 Unlike VGLUT1 and VGLUT2, which are almost exclusively present in nerve endings,
595 VGLUT3 is present in both terminals and neuronal cell bodies (Gras et al., 2002; Somogyi et
596 al., 2004). We, therefore, studied the cellular and subcellular distribution of VGLUT3-
597 p.A224V in these cellular compartments (Fig. 5). The expression of VGLUT3-p.A224V was
598 dramatically reduced in terminals from the striatum or hippocampus (CA1) compared with
599 WT levels (Fig. 5A, B, C, striatum: -69%, Mann-Whitney U test, $p < 0.0001$, $n = 19$; Fig. 5E,
600 F, G, hippocampus: -72%, Mann-Whitney U test, $p < 0.0001$, $n = 20$; 8 animals per
601 genotype). However, surprisingly, VGLUT3 levels were similar in the soma of tonically active
602 cholinergic interneurons (TANs) and the hippocampal basket cells from WT and
603 VGLUT3^{A224V/A224V} mice (Fig. 5D, H, Mann-Whitney U test, $p > 0.05$). Furthermore, using
604 electron microscopy, we observed that in TANs, the WT as well as the VGLUT3-p.A224V
605 isoforms were distributed over similar subcellular organelles, including the endoplasmic
606 reticulum (Fig. 5I, J; $n = 5$ for each genotype). Together, these data suggest that the
607 VGLUT3-p.A224V isoform is not abnormally accumulated in the soma of neurons and that its
608 expression is markedly reduced in terminals.

609 The mobility of VGLUT3-p.A211V is minimally modified

610 The aforementioned results suggested that VGLUT3-p.A211V was either not properly
611 trafficked or was degraded in the nerve endings. To test the first hypothesis, we used
612 fluorescence recovery after photobleaching (FRAP) to assess the mobility of VGLUT3 WT or
613 VGLUT3-p.A211V in synaptic boutons, as previously described (Herzog et al., 2011).
614 Hippocampal neurons were transduced at 2 DIV with a lentiviral vector expressing either the
615 WT isoform of VGLUT3 or VGLUT3-p.A211V; both were tagged with the YFP derivative
616 venus (Fig. 6A). VGLUT3-p.A211V transduction was adjusted to match the expression level
617 of WT VGLUT3. Transduction of both isoforms yielded a punctate distribution of venus
618 fluorescence that was reminiscent of presynaptic localization. A bleaching light pulse was
619 applied to regions of interest (ROI) surrounding individual boutons in mature neurons after 17
620 days in culture (Fig. 6A). The exchange of bleached synaptic vesicles (SVs) and
621 fluorescently labeled SVs from neurites surrounding the ROI was monitored during the next
622 75 minutes (Fig. 6A). VGLUT3-p.A211V fluorescence recovered to levels similar to those of
623 the wild-type protein (Fig. 6A, B). An additional FRAP experiment with faster imaging rates in
624 the first five minutes was performed to reveal possible differences in the initial recovery
625 phase (Fig. 6B, fast FRAP inset). The kinetics of recovery seemed slightly different, but these
626 differences were not statistically significant. However, the amplitude of recovery at 1 hour
627 was similar for the mutant and wild-type experiments (Fig. 6C, Mann Whitney U test, $p =$
628 0.1129). Therefore, although we cannot rule out that the mobility of the over-expressed
629 venus-tagged VGLUT3-p.A211V mutant isoform was altered, we conclude that the p.A211V
630 mutation powerfully reduces VGLUT3 expression in terminals without apparently altering its
631 mobility. .

632

633 The p.A224V mutation does not alter the behavior of mutant mice

634 Mice lacking VGLUT3 (VGLUT3^{-/-}) demonstrate increased anxiety behavior, as well as
635 augmented basal and cocaine-induced locomotor activity (Gras et al., 2008; Amilhon et al.,
636 2010; Sakae et al., 2015). We thus decided to characterize these behaviors in adult (3-4-

637 month-old) male VGLUT3^{A224V/A224V} mice with only 30% VGLUT3 expression. We first
638 assessed the anxiety levels of WT and mutant animals in an open field and an elevated plus
639 maze (Fig. 7A, B). Spontaneous as well as cocaine-induced locomotor activities were also
640 measured (Fig. 7C, D). No significant differences between WT and VGLUT3^{A224V/A224V} mice
641 were observed in any paradigm. Therefore, the p.A211V mutation does not modify VGLUT3-
642 dependent mood or locomotor phenotypes.

643 We next investigated the behavior of VGLUT3^{A224V/-} mice that displayed a 78% reduction of
644 VGLUT3 expression. We first compared the anxiety behaviors of WT and VGLUT3^{A224V/-}
645 mice in the open field and elevated plus maze and found no differences (Fig. 7E, F). We then
646 inspected basal and cocaine-induced locomotor activity of WT and VGLUT3^{A224V/-} mice (Fig.
647 7G, H). During the first two hours, we recorded the basal locomotor activity of mutant and
648 WT mice and observed a significant increase in the activity in VGLUT3^{A224V/-} mice (Fig. 7G,
649 repeated-measures ANOVA, $F_{(1, 29)}=1.472$, $p < 0.05$; *H*, cumulative analysis, +41%, Mann-
650 Whitney U test, $p = 0.0329$). In contrast, the locomotor activity levels after cocaine injection
651 were similar in both genotypes (Fig. 7H, Mann-Whitney U test, $p > 0.05$). Therefore, with only
652 one copy of the VGLUT3-p.A224V isoform, and only 20% VGLUT3 expression, we detected
653 minimal alterations in mutant mice behavior.

654

655 **The p.A224V point mutation does not modify VGLUT3-dependent vesicular synergy** 656 **over cortical [³H]5-HT accumulation**

657 We then investigated whether the p.A224V mutation was able to alter the vesicular
658 accumulation of glutamate in brain SVs of VGLUT3 mutants. VGLUT3 is a minor subtype
659 compared with VGLUT1 and VGLUT2. It is therefore not possible to directly assess VGLUT3
660 activity in brain tissue. However, it has been previously established that VGLUT3 accelerates
661 5-HT accumulation in cortical synaptic vesicles through a molecular process called vesicular
662 synergy (Amilhon et al., 2010; El Mestikawy et al., 2011). To estimate VGLUT3 activity in
663 cortical synaptic vesicles, reserpine-sensitive vesicular uptake of [³H]5-HT was measured in
664 the presence (+) or absence (-) of L-glutamate (Fig. 8). Similarly to previously reported

665 results (Amilhon et al., 2010), L-glutamate (10 mM) increased [³H]5-HT reserpine-sensitive
666 accumulation by 27% (Fig. 8, Mann-Whitney U test, $p < 0.0001$, $n = 26$) in the cortical
667 synaptic vesicles of WT mice but had no effect on those of VGLUT3^{-/-} mice. Similarly to the
668 results for WT mice, we observed a vesicular synergy in 5-HT vesicular uptake of +27% in
669 VGLUT3^{A224V/+} mice (Mann-Whitney U test, $p = 0.0014$, $n = 7$), +22% in VGLUT3^{A224V/A224V}
670 mice (Mann-Whitney U test, $p < 0.0001$, $n = 19$) and +22% in VGLUT3^{A224V/-} mice (Mann-
671 Whitney U test, $p < 0.001$, $n = 19$). The stimulatory effect of glutamate on 5-HT cortical
672 vesicular uptake was not significantly different between the WT and the three other
673 genotypes (one-way ANOVA, $p > 0.05$). We conclude from these experiments that VGLUT3
674 activity was probably unaltered, even in mice with only 20-30% transporter expression.

675

676 **High resolution fluorescence microscopy suggests that the p.A224V mutation alters**
677 **the number of VGLUT3-positive vesicles**

678 The aforementioned results strongly suggested that the p.A224V mutation markedly reduces
679 the number of copies of VGLUT3 in synaptic boutons. This decrease in copy number may
680 result in i) a reduction in the number of copies of the transporter on each vesicle or/and ii) a
681 reduction in the number of VGLUT3-positive vesicles in each terminal. In an attempt to gain
682 further insight in this issue, we used STED super resolution imaging of VGLUT3 in the
683 striatum of mutant mice (Fig. 9).

684 STED microscopic observations after immunodetection showed spotty labeling of VGLUT3 and
685 synaptophysin (Fig. 9A-E). The number of VGLUT3-positive puncta was highest in WT mice,
686 was virtually nonexistent in VGLUT3^{-/-} mice and was decreased in VGLUT3^{A224V/+},
687 VGLUT3^{A224V/A224V} and VGLUT3^{A224V/-} mice. The quantification of VGLUT3 immunopositive
688 puncta revealed decreases of: 45% (Kruskal-Wallis test, $p = 0.0029$), 75% (Kruskal-Wallis test, p
689 $= 0.0022$) and 84% (Kruskal-Wallis test, $p = 0.0022$) in VGLUT3^{A224V/+}, VGLUT3^{A224V/A224V} and
690 VGLUT3^{A224V/-} mice, respectively (Fig. 9F). These decreases were significantly correlated with
691 the expression of VGLUT3 detected by immunoautoradiography (Fig. 9G, linear regression, $r^2 =$
692 0.9528 , $p = 0.0044$). In contrast, the expression of synaptophysin was found to be similar in WT

693 and in the panel of VGLUT3 mutants (Fig. 9*F*). Interestingly, increasing laser power neither
694 increased the number of detected puncta (Fig. 9*H*, Kruskal-Wallis test, $p > 0.05$) nor allowed the
695 detection of a population of puncta with low intensity labeling.
696 Therefore, although it was not possible to determine whether the number of VGLUT3 copy
697 per vesicle was reduced, STED imaging suggested that diminishing the expression of
698 VGLUT3 reduced the number of VGLUT3-positive vesicles.
699

700 **DISCUSSION**

701

702 In two human families, a point mutation in the gene encoding VGLUT3 exchanges the amino
703 acid alanine 211 for a valine and segregates with an early onset form of presbycusis (named
704 DFNA25, (Ruel et al., 2008)). The VGLUT3-p.A211V (VGLUT3-p.A224V in rodent) point
705 mutation is the first identified mutation of a VGLUT that is responsible for a human pathology.
706 The impact of this mutation on the auditory system of the rodent is currently under
707 investigation. Our preliminary results show that the p.A224V mutation recapitulates the
708 human auditory pathology (Miot et al., manuscript in preparation). The aim of the present
709 study was to determine whether and how the p.A211V mutation influences CNS activity.
710 Consequently, functions of mutant VGLUT3 were investigated in cell cultures, as well as in a
711 genetic mouse model.

712 Interestingly, alanine 211 is part of a peptide sequence (KWAPPLER) that is conserved
713 among VGLUTs and is even present in the more distant transporter named sialin. According
714 to a theoretical model (Fig. 3A-H), the KWAPPLER motif is part of a small cytoplasmic loop
715 that faces the pore of the transporter. Both the conservation and the localization of alanine
716 211 argue for its functional importance. Structurally, our 3D model predicted that exchanging
717 alanine for valine would have little influence on the structure of VGLUT3. In line with this
718 conclusion, glutamate vesicular accumulation in BON cells and evoked EPSCs observed in
719 isolated neuronal cultures expressing the VGLUT3-p.A211V isoform were not different from
720 that observed with the WT isoform. Furthermore, indirect estimation of VGLUT3 activity in
721 cortical synaptic vesicles provided evidence that the ability of VGLUT3 to load glutamate in
722 vesicles was not different in the brains of WT or mutant mice.

723 However, in both cell cultures and in a mutant mouse model, the mutation had a dramatic
724 effect on the expression of the transporter. The average decrease across investigated brain
725 areas of the mutant transporter in VGLUT3^{A224V/A224V} mice was $70 \pm 2.7\%$. As expected, mice
726 with a single copy of the mutated allele (VGLUT3^{A224V/-}) express $\approx 15\text{-}20\%$ of transporter
727 whereas those with 2 copies (VGLUT3^{A224V/A224V}) express $\approx 20\text{-}30\%$ of transporter (Table II).

728 These decreases could impact more severely synapses expressing low levels of VGLUT3. It
729 thus cannot be ruled out that the VGLUT3-p.A221V mutation could have stronger effects in
730 some terminals present in non-inspected brain regions.

731 In the mutant mouse brain, the impact of the mutation on the expression of VGLUT3 appears
732 to be constant between P10 and 12-month-old. This observation suggests that the reduction
733 of VGLUT3 triggered by the mutation is independent from aging. Interestingly when the
734 equivalent alanine in VGLUT1 (Alanine 198) was mutated into a valine residue, an even
735 stronger decrease of the transporter was observed (-90%; Fig. 2F). Therefore, alanine in the
736 KWAPPLER motif could be pivotal for the expression levels (or stability) of all VGLUTs.

737 In VGLUT3^{A224V/A224V} mice, the amount of the mutant transporter was dramatically reduced in
738 hippocampal, striatal and cortical terminals. However, this point mutation had no effect on the
739 mRNA or on protein levels in the soma and proximal dendrites of VGLUT3-positive neurons.
740 This result implies that the mutation does not alter the transcription or translation of VGLUT3.
741 Furthermore, the mobility of VGLUT3-p.A211V was not significantly modified in the axons.
742 These results suggested that the mutant transporter could be less stable or more rapidly
743 degraded in the terminals of neurons. However, it should be kept in mind that the expression
744 of mutant VGLUT3 was as low in BON as in primary neurons or in the mouse brain. Further
745 investigation of the half-life of the mutated isoform will be needed to clarify this issue.

746 We estimated the activity of the mutated isoform directly by measuring glutamate uptake in
747 vesicles of BON cells and indirectly by measuring synaptic transmission in single neurons
748 expressing the mutant transporter or by measuring vesicular synergy in cortical vesicles. In
749 all cases, we found very minimal or no modifications of VGLUT3 activity.

750 A previous study reported that in *Caenorhabditis elegans*, 4 different point mutations of
751 VACHT profoundly altered transporter activity (mostly the Km) without decreasing its
752 expression or altering its targeting (Zhu et al., 2001). This illustrates the complex and diverse
753 effects of point mutations on transporters activity.

754 Previous reports established that mice completely lacking VGLUT3 demonstrate increased
755 anxiety and sensitivity to cocaine (Gras et al., 2008; Amilhon et al., 2010; Sakae et al., 2015).

756 Here, none of these phenotypes were observed with VGLUT3^{A224V/A224V} mice lacking more
757 than 70% of VGLUT3, and only moderate effects were observed on locomotor activity in a
758 mutant lacking up to 80% of VGLUT3 (VGLUT3^{A224V/-}). Our results showed that despite a
759 substantial reduction in VGLUT3 expression, its biochemical and many integrated functions
760 were unchanged. However, we cannot rule out that VGLUT3^{A224V/A224V} or VGLUT3^{A224V/+} mice
761 may display some phenotypes that were not investigated in the present study. For example,
762 mice lacking VGLUT3 demonstrate abnormal interictal discharges (Seal et al., 2008). These
763 cortical generalized synchronous discharges are not accompanied by convulsive
764 electrographic seizures. Interestingly, knock-out mice heterozygous for VGLUT3 (VGLUT3^{+/-})
765 also show sharp interictal spike discharges. We therefore cannot exclude the possibility that
766 VGLUT3^{A224V/A224V} or VGLUT3^{A224V/+} mice present the abnormal interictal discharges reported
767 in VGLUT3^{+/-} mice (Seal et al., 2008).

768 Nonetheless for phenotypes such as locomotor activity, sensitivity to cocaine or anxiety
769 VGLUT3^{A224V/A224V} or VGLUT3^{A224V/+} mice demonstrated no behavioral alterations. As
770 depicted in the model in Fig. 10A, there may be a substantial safety factor in the level of
771 VGLUT3 required to sustain glutamate uptake such that only a small copy number is
772 required to maintain these physiological functions. The threshold where a decrease of
773 VGLUT3 level will start to impact its function is situated within a narrow range between 20
774 and 0% of wild-type level (Fig. 10A). Therefore, unlike those of the monoamine and
775 acetylcholine vesicular transporters, VMAT2 and VACHT (Fon et al., 1997; Prado et al.,
776 2006), the safety factor for VGLUT3 may be higher, with normal function being maintained,
777 even with protein levels that are below 70% of WT levels.

778 A key question is whether these observations are also valid for VGLUT1 and VGLUT2.
779 Whether vesicular accumulation of glutamate catalyzed by VGLUT1 or VGLUT2 is
780 proportional to the amount of transporters has been a matter of debate (for review see
781 (Schuske and Jorgensen, 2004) and (Freneau et al., 2004; Wojcik et al., 2004; Wilson et al.,
782 2005)). Wojcik et al. have reported decreases in mEPSC amplitude and frequency in
783 neurons lacking VGLUT1, and conversely, increased quantal size in neurons over-

784 expressing VGLUT1 (Wojcik et al., 2004). Furthermore, Wilson et al. reported that in
785 hippocampal neuronal culture as well as during postnatal development, increasing the
786 density of VGLUT1 results in enhanced glutamate release into the synaptic cleft (Wilson et
787 al., 2005). These observations support a linear relationship between VGLUT1 amount and
788 VGLUT1 activity (i.e. glutamate vesicular packaging). However, if glutamate vesicular loading
789 and transmission were proportional to the copy number of VGLUTs, then heterozygous
790 knockout mice (with 50% VGLUT expression) should display a 50% decrease in
791 glutamatergic signaling, and this, in turn, should impact related behaviors. Fremeau et al.
792 showed that VGLUT1^{+/-} heterozygous mice display normal excitatory transmission (Fremeau
793 et al., 2004). In contrast, impaired mood regulation and memory have been reported in
794 VGLUT1^{+/-} heterozygous mice (Tordera et al., 2007; Balschun et al., 2010). VGLUT2^{+/-} mice
795 express only 50% of the WT level but demonstrate only discrete phenotypes in taste
796 aversion, nociceptive responses and clonic seizures (Moechars et al., 2006; Leo et al., 2009;
797 Schallier et al., 2009). However, these phenotypes are often modest.

798 Takamori and coworkers showed that, on average, synaptic vesicles contain 10 copies of
799 VGLUT1 or 14 copies of VGLUT2 protein (Takamori et al., 2006). Hence, there are multiple
800 copies of VGLUT1-2 inserted into vesicular membranes. The exact number of copies of
801 VGLUT3 that are present on individual synaptic vesicles has not yet been determined.
802 However, it can be reasonably assumed that, as with VGLUT1 and VGLUT2, multiple copies
803 of VGLUT3 are inserted in the membrane of synaptic vesicles.

804 The redundancy of vesicular glutamate copies per vesicles could provide a safety factor in
805 case of loss of transporters. For example, in *Drosophila*, reduced levels of DVGLUTs result
806 in a reduction of mEPSC frequency, with no change in quantal size (Daniels et al., 2006).
807 Additional studies support the notion that one copy of a VGLUT is sufficient to fill synaptic
808 vesicles and to maintain a normal quantal size (Wojcik et al., 2004; Daniels et al., 2006;
809 Schenck et al., 2009; Preobraschenski et al., 2014), as depicted in Model 1 (Fig 10A). Model
810 1 predicts that the decreased expression of VGLUT3-p.A224V could be due to a
811 homogeneous reduction of the number of copies of transporter per vesicles. According to this

812 model, as long as there is at least 20% residual VGLUT3, the filling of vesicles with
813 glutamate should be normal. The exact number of copies of VGLUT3 per vesicle
814 corresponding to this percentage remains to be determined.

815 In the present study, we observed normal loading of [³H]L-glutamate into VGLUT3-p.A211V
816 positive BON vesicles. However, a small significant decrease in mEPSC amplitude was
817 observed in isolated neurons expressing the mutant isoform. It should be noted that
818 electrophysiological recordings in autapses were obtained with increased amounts of mutant
819 isoform with the objective of normalizing levels with those of the WT isoform. This represents
820 a limitation of the present study as studying the effects of the mutation on synaptic activity
821 without artificially increasing the level of the mutant transporter may have better represented
822 the situation occurring in mutation carriers. Discrepancies between vesicular uptake and
823 electrophysiological measurements can easily be explained by a difference in the sensitivity
824 of both methods. In line with this explanation, a small but non-significant decrease was
825 observed in vesicles of BON cells expressing VGLUT3-p.A211V. However, Model 1 does not
826 explain why a significant decrease of mEPSC frequency was observed in isolated neurons
827 expressing the mutant isoform. Furthermore, this model is not readily compatible with our
828 observations obtained by STED microscopy. Surprisingly, STED showed a decrease of
829 VGLUT3-positive fluorescent puncta per terminal. This suggests that the reduced expression
830 of the mutated isoform in terminals is due to a reduction of the number of VGLUT3-positive
831 vesicles as described by Model 2.

832 This second model is well in line with the decreased frequency of mEPSC observed in
833 hippocampal autapses expressing VGLUT3-p.A211V. Indeed an increased number of
834 “empty” vesicles could result in an increased number of silent events and therefore in a
835 decreased frequency of mEPSCs. However, Model 2 is not compatible with the fact that
836 vesicular uptake (in BON cells and in brain vesicles) and release probability (in hippocampal
837 autapses) were virtually unchanged.

838 The discrepancy between the predictions of models 1 and 2 could be resolved if there is a
839 non-homogeneous distribution of the mutant isoform between different pools of vesicles as

840 shown with Model 3. In this third putative model, we propose the existence of at least 3
841 populations of synaptic vesicles in VGLUT3^{A224V/A224V} mice. Synaptic vesicles could contain
842 either high (or normal) or low level VGLUT3-p.A224V copies. Synaptic vesicles with a low
843 copy number of mutant VGLUT3 would not be detected by STED microscopy. They could
844 contain a slightly decreased amount of glutamate therefore explaining the small decrease in
845 the amplitude of mEPSCs in hippocampal autapses. The vesicular populations with “high and
846 low” VGLUT3-p.A211V content could allow a normal or only slightly altered quantum of
847 glutamate. They also could explain why VGLUT3 biochemical, electrophysiological and
848 behavioral function are preserved in VGLUT3^{A224V/A224V} mice. In addition a small fraction of
849 synaptic vesicles are present with no copy of VGLUT3-p.A221V. These vesicles account for
850 the decreased frequency of mEPSC depicted in Fig 3P and Q. If this model is correct, it
851 implies that the KWAPPLER motif plays a central role in the vesicular targeting of VGLUT3.
852 In particular, the trafficking of VGLUT3-p.A211V between different vesicular pools appears to
853 be profoundly altered. Interestingly, synaptophysin labeling remained constant in the various
854 VGLUT3 mutant mice analyzed in this study. This observation suggests that the number of
855 synaptic vesicles is unaltered in the mutant mice.

856 The validation or invalidation of Model 3 will necessitate further experiments such as the use
857 of super-resolution microscopic approaches (STORM or PALM). These methods that allow
858 detection of single molecules may help to quantify the number of VGLUT3 per vesicle.

859 Rare variants of VGLUTs have begun to be identified in human pathologies (Ruel et al.,
860 2008; Shen et al., 2010; Sakae et al., 2015). It is a key challenge to understand how these
861 mutations can affect VGLUT functions and glutamatergic transmission. As shown here, the
862 A224V mutation that causes deafness in humans profoundly alters the protein levels of
863 VGLUT3, but minimally alters its functions. Our study reveals an unexpected redistribution of
864 VGLUT3 in the synaptic vesicles of VGLUT3^{A224V/A224V} mice brain. Furthermore, we suggest
865 the existence of a large safety factor in the number of VGLUT3 molecules required to sustain
866 normal physiological functions. Further experiments will be required to validate or invalidate
867 the three models proposed in Fig. 10. Clarifying this question will be important for gaining a

868 complete understanding of the pathologies that involve VGLUTs.

869 **REFERENCES**

- 870
871 Almqvist J, Huang Y, Laaksonen A, Wang DN, Hovmoller S (2007) Docking and homology
872 modeling explain inhibition of the human vesicular glutamate transporters. *Protein Sci*
873 16:1819-1829.
- 874 Amilhon B, Lepicard E, Renoir T, Mongeau R, Popa D, Poirel O, Miot S, Gras C, Gardier AM,
875 Gallego J, Hamon M, Lanfumey L, Gasnier B, Giros B, El Mestikawy S (2010) VGLUT3
876 (vesicular glutamate transporter type 3) contribution to the regulation of serotonergic
877 transmission and anxiety. *J Neurosci* 30:2198-2210.
- 878 Balschun D, Moechars D, Callaerts-Vegh Z, Vermaercke B, Van Acker N, Andries L,
879 D'Hooge R (2010) Vesicular glutamate transporter VGLUT1 has a role in hippocampal long-
880 term potentiation and spatial reversal learning. *Cereb Cortex* 20:684-693.
- 881 Bellocchio EE, Reimer RJ, Fremeau RT, Edwards RH (2000) Uptake of glutamate into
882 synaptic vesicles by an inorganic phosphate transporter. *Science* 289:957-960.
- 883 Bernard V, Levey AI, Bloch B (1999) Regulation of the subcellular distribution of m4
884 muscarinic acetylcholine receptors in striatal neurons in vivo by the cholinergic environment:
885 evidence for regulation of cell surface receptors by endogenous and exogenous stimulation.
886 *J Neurosci* 19:10237-10249.
- 887 Daniels RW, Miller BR, DiAntonio A (2011) Increased vesicular glutamate transporter
888 expression causes excitotoxic neurodegeneration. *Neurobiol Dis* 41:415-420.
- 889 Daniels RW, Collins CA, Chen K, Gelfand MV, Featherstone DE, DiAntonio A (2006) A single
890 vesicular glutamate transporter is sufficient to fill a synaptic vesicle. *Neuron* 49:11-16.
- 891 Daniels RW, Collins CA, Gelfand MV, Dant J, Brooks ES, Krantz DE, DiAntonio A (2004)
892 Increased expression of the *Drosophila* vesicular glutamate transporter leads to excess
893 glutamate release and a compensatory decrease in quantal content. *J Neurosci* 24:10466-
894 10474.
- 895 De Gois S, Slama P, Pietrancosta N, Erdozain AM, Louis F, Bouvrais-Veret C, Daviet L,
896 Giros B (2015) Ctr9, a Protein in the Transcription Complex Paf1, Regulates Dopamine
897 Transporter Activity at the Plasma Membrane. *J Biol Chem* 290:17848-17862.
- 898 El Mestikawy S, Wallen-Mackenzie A, Fortin GM, Descarries L, Trudeau LE (2011) From
899 glutamate co-release to vesicular synergy: vesicular glutamate transporters. *Nat Rev*
900 *Neurosci* 12:204-216.
- 901 Fasano C, Thibault D, Trudeau LE (2008) Culture of postnatal mesencephalic dopamine
902 neurons on an astrocyte monolayer. *Curr Protoc Neurosci* Chapter 3:Unit 3 21.
- 903 Feyfant E, Sali A, Fiser A (2007) Modeling mutations in protein structures. *Protein Sci*
904 16:2030-2041.

905 Fon EA, Pothos EN, Sun BC, Killeen N, Sulzer D, Edwards RH (1997) Vesicular transport
906 regulates monoamine storage and release but is not essential for amphetamine action.
907 *Neuron* 19:1271-1283.

908 Fremeau RT, Troyer MD, Pahner I, Nygaard GO, Tran CH, Reimer RJ, Bellocchio EE, Fortin
909 D, Storm-Mathisen J, Edwards RH (2001) The expression of vesicular glutamate transporters
910 defines two classes of excitatory synapse. *Neuron* 31:247-260.

911 Fremeau RT, Burman J, Qureshi T, Tran CH, Proctor J, Johnson J, Zhang H, Sulzer D,
912 Copenhagen DR, Storm-Mathisen J, Reimer RJ, Chaudhry FA, Edwards RH (2002) The
913 identification of vesicular glutamate transporter 3 suggests novel modes of signaling by
914 glutamate. *Proc Natl Acad Sci U S A* 99:14488-14493.

915 Fremeau RT, Jr., Kam K, Qureshi T, Johnson J, Copenhagen DR, Storm-Mathisen J,
916 Chaudhry FA, Nicoll RA, Edwards RH (2004) Vesicular glutamate transporters 1 and 2 target
917 to functionally distinct synaptic release sites. *Science* 304:1815-1819.

918 Gras C, Herzog E, Bellenchi GC, Bernard V, Ravassard P, Pohl M, Gasnier B, Giros B, El
919 Mestikawy S (2002) A third vesicular glutamate transporter expressed by cholinergic and
920 serotonergic neurons. *J Neurosci* 22:5442-5451.

921 Gras C, Amilhon B, Lepicard EM, Poirel O, Vinatier J, Herbin M, Dumas S, Tzavara ET,
922 Wade MR, Nomikos GG, Hanoun N, Saurini F, Kemel ML, Gasnier B, Giros B, El Mestikawy
923 S (2008) The vesicular glutamate transporter VGLUT3 synergizes striatal acetylcholine tone.
924 *Nat Neurosci* 11:292-300.

925 Herman MA, Ackermann F, Trimbuch T, Rosenmund C (2014) Vesicular glutamate
926 transporter expression level affects synaptic vesicle release probability at hippocampal
927 synapses in culture. *J Neurosci* 34:11781-11791.

928 Herzog E, Gilchrist J, Gras C, Muzerelle A, Ravassard P, Giros B, Gaspar P, El Mestikawy S
929 (2004) Localization of VGLUT3, the vesicular glutamate transporter type 3, in the rat brain.
930 *Neuroscience* 123:983-1002.

931 Herzog E, Bellenchi GC, Gras C, Bernard V, Ravassard P, Bedet C, Gasnier B, Giros B, El
932 Mestikawy S (2001) The existence of a second vesicular glutamate transporter specifies
933 subpopulations of glutamatergic neurons. *J Neurosci* 21:RC181.

934 Herzog E, Nadrigny F, Silm K, Biesemann C, Helling I, Bersot T, Steffens H, Schwartzmann
935 R, Nöckerl UV, El Mestikawy S, Rhee J, Kirchhoff F, Brose N (2011) In vivo imaging of
936 intersynaptic vesicle exchange using VGLUT1 Venus knock-in mice. *J Neurosci* 31:15544-
937 15559.

938 Higley MJ, Gittis AH, Oldenburg IA, Balthasar N, Seal RP, Edwards RH, Lowell BB, Kreitzer
939 AC, Sabatini BL (2011) Cholinergic interneurons mediate fast VGLUT3-dependent
940 glutamatergic transmission in the striatum. *PLoS One* 6:e19155.

- 941 Krogh A, Larsson B, von Heijne G, Sonnhammer EL (2001) Predicting transmembrane
942 protein topology with a hidden Markov model: application to complete genomes. *J Mol Biol*
943 305:567-580.
- 944 Leo S, Moechars D, Callaerts-Vegh Z, D'Hooge R, Meert T (2009) Impairment of VGLUT2
945 but not VGLUT1 signaling reduces neuropathy-induced hypersensitivity. *Eur J Pain* 13:1008-
946 1017.
- 947 McAnaney TB, Zeng W, Doe CF, Bhanji N, Wakelin S, Pearson DS, Abbyad P, Shi X, Boxer
948 SG, Bagshaw CR (2005) Protonation, photobleaching, and photoactivation of yellow
949 fluorescent protein (YFP 10C): a unifying mechanism. *Biochemistry* 44:5510-5524.
- 950 Moechars D, Weston MC, Leo S, Callaerts-Vegh Z, Goris I, Daneels G, Buist A, Cik M, van
951 der Spek P, Kass S, Meert T, D'Hooge R, Rosenmund C, Hampson RM (2006) Vesicular
952 glutamate transporter VGLUT2 expression levels control quantal size and neuropathic pain. *J*
953 *Neurosci* 26:12055-12066.
- 954 Nelson AB, Bussert TG, Kreitzer AC, Seal RP (2014) Striatal cholinergic neurotransmission
955 requires VGLUT3. *J Neurosci* 34:8772-8777.
- 956 Peirs C, Williams SP, Zhao X, Walsh CE, Gedeon JY, Cagle NE, Goldring AC, Hioki H, Liu Z,
957 Marell PS, Seal RP (2015) Dorsal Horn Circuits for Persistent Mechanical Pain. *Neuron*
958 87:797-812.
- 959 Prado VF et al. (2006) Mice deficient for the vesicular acetylcholine transporter are
960 myasthenic and have deficits in object and social recognition. *Neuron* 51:601-612.
- 961 Preobraschenski J, Zander JF, Suzuki T, Ahnert-Hilger G, Jahn R (2014) Vesicular
962 glutamate transporters use flexible anion and cation binding sites for efficient accumulation of
963 neurotransmitter. *Neuron* 84:1287-1301.
- 964 Rosenmund C, Stevens CF (1996) Definition of the readily releasable pool of vesicles at
965 hippocampal synapses. *Neuron* 16:1197-1207.
- 966 Ruel J, Emery S, Nouvian R, Bersot T, Amilhon B, Van Rybroek JM, Rebillard G, Lenoir M,
967 Eybalin M, Delprat B, Sivakumaran TA, Giros B, El Mestikawy S, Moser T, Smith RJ,
968 Lesperance MM, Puel JL (2008) Impairment of SLC17A8 encoding vesicular glutamate
969 transporter-3, VGLUT3, underlies nonsyndromic deafness DFNA25 and inner hair cell
970 dysfunction in null mice. *Am J Hum Genet* 83:278-292.
- 971 Sakae DY et al. (2015) The absence of VGLUT3 predisposes to cocaine abuse by increasing
972 dopamine and glutamate signaling in the nucleus accumbens. *Mol Psychiatry*.
- 973 Schafer MK, Varoqui H, Defamie N, Weihe E, Erickson JD (2002) Molecular cloning and
974 functional identification of mouse vesicular glutamate transporter 3 and its expression in
975 subsets of novel excitatory neurons. *J Biol Chem* 277:50734-50748.

- 976 Schallier A, Massie A, Loyens E, Moechars D, Drinkenburg W, Michotte Y, Smolders I (2009)
977 vGLUT2 heterozygous mice show more susceptibility to clonic seizures induced by
978 pentylenetetrazol. *Neurochem Int* 55:41-44.
- 979 Schenck S, Wojcik SM, Brose N, Takamori S (2009) A chloride conductance in VGLUT1
980 underlies maximal glutamate loading into synaptic vesicles. *Nat Neurosci* 12:156-162.
- 981 Schuske K, Jorgensen EM (2004) Neuroscience. Vesicular glutamate transporter--shooting
982 blanks. *Science* 304:1750-1752.
- 983 Seal RP, Wang X, Guan Y, Raja SN, Woodbury CJ, Basbaum AI, Edwards RH (2009) Injury-
984 induced mechanical hypersensitivity requires C-low threshold mechanoreceptors. *Nature*
985 462:651-655.
- 986 Seal RP, Akil O, Yi E, Weber CM, Grant L, Yoo J, Clause A, Kandler K, Noebels JL,
987 Glowatzki E, Lustig LR, Edwards RH (2008) Sensorineural deafness and seizures in mice
988 lacking vesicular glutamate transporter 3. *Neuron* 57:263-275.
- 989 Shen YC, Liao DL, Lu CL, Chen JY, Liou YJ, Chen TT, Chen CH (2010) Resequencing of
990 the vesicular glutamate transporter 2 gene (VGLUT2) reveals some rare genetic variants that
991 may increase the genetic burden in schizophrenia. *Schizophr Res* 121:179-186.
- 992 Siksou L, Silm K, Biesemann C, Nehring RB, Wojcik SM, Triller A, El Mestikawy S, Marty S,
993 Herzog E (2013) A role for vesicular glutamate transporter 1 in synaptic vesicle clustering
994 and mobility. *Eur J Neurosci* 37:1631-1642.
- 995 Somogyi J, Baude A, Omori Y, Shimizu H, El Mestikawy S, Fukaya M, Shigemoto R,
996 Watanabe M, Somogyi P (2004) GABAergic basket cells expressing cholecystokinin contain
997 vesicular glutamate transporter type 3 (VGLUT3) in their synaptic terminals in hippocampus
998 and isocortex of the rat. *Eur J Neurosci* 19:552-569.
- 999 Takamori S, Rhee JS, Rosenmund C, Jahn R (2000) Identification of a vesicular glutamate
1000 transporter that defines a glutamatergic phenotype in neurons. *Nature* 407:189-194.
- 1001 Takamori S, Rhee JS, Rosenmund C, Jahn R (2001) Identification of differentiation-
1002 associated brain-specific phosphate transporter as a second vesicular glutamate transporter
1003 (VGLUT2). *J Neurosci* 21:RC182.
- 1004 Takamori S, Malherbe P, Broger C, Jahn R (2002) Molecular cloning and functional
1005 characterization of human vesicular glutamate transporter 3. *EMBO Rep* 3:798-803.
- 1006 Takamori S et al. (2006) Molecular anatomy of a trafficking organelle. *Cell* 127:831-846.
- 1007 Thompson JD, Higgins DG, Gibson TJ (1994) CLUSTAL W: improving the sensitivity of
1008 progressive multiple sequence alignment through sequence weighting, position-specific gap
1009 penalties and weight matrix choice. *Nucleic Acids Res* 22:4673-4680.
- 1010 Tordera RM, Totterdell S, Wojcik SM, Brose N, Elizalde N, Lasheras B, Del Rio J (2007)
1011 Enhanced anxiety, depressive-like behaviour and impaired recognition memory in mice with

1012 reduced expression of the vesicular glutamate transporter 1 (VGLUT1). *Eur J Neurosci*
1013 25:281-290.

1014 Tusnady GE, Simon I (2001) The HMMTOP transmembrane topology prediction server.
1015 *Bioinformatics* 17:849-850.

1016 Varga V, Losonczy A, Zemelman BV, Borhegyi Z, Nyiri G, Domonkos A, Hangya B, Holderith
1017 N, Magee JC, Freund TF (2009) Fast synaptic subcortical control of hippocampal circuits.
1018 *Science* 326:449-453.

1019 Varoqui H, Schafer MK, Zhu H, Weihe E, Erickson JD (2002) Identification of the
1020 differentiation-associated Na⁺/PI transporter as a novel vesicular glutamate transporter
1021 expressed in a distinct set of glutamatergic synapses. *J Neurosci* 22:142-155.

1022 Vigneault E, Poirel O, Riad M, Prud'homme J, Dumas S, Turecki G, Fasano C, Mechawar N,
1023 El Mestikawy S (2015) Distribution of vesicular glutamate transporters in the human brain.
1024 *Front Neuroanat* 9:23.

1025 Weston MC, Nehring RB, Wojcik SM, Rosenmund C (2011) Interplay between VGLUT
1026 isoforms and endophilin A1 regulates neurotransmitter release and short-term plasticity.
1027 *Neuron* 69:1147-1159.

1028 Wilson NR, Kang J, Hueske EV, Leung T, Varoqui H, Murnick JG, Erickson JD, Liu G (2005)
1029 Presynaptic regulation of quantal size by the vesicular glutamate transporter VGLUT1. *J*
1030 *Neurosci* 25:6221-6234.

1031 Wojcik SM, Rhee JS, Herzog E, Sigler A, Jahn R, Takamori S, Brose N, Rosenmund C
1032 (2004) An essential role for vesicular glutamate transporter 1 (VGLUT1) in postnatal
1033 development and control of quantal size. *Proc Natl Acad Sci U S A* 101:7158-7163.

1034 Zander JF, Munster-Wandowski A, Brunk I, Pahner I, Gomez-Lira G, Heinemann U,
1035 Gutierrez R, Laube G, Ahnert-Hilger G (2010) Synaptic and vesicular coexistence of VGLUT
1036 and VGAT in selected excitatory and inhibitory synapses. *J Neurosci* 30:7634-7645.

1037 Zhu H, Duerr JS, Varoqui H, McManus JR, Rand JB, Erickson JD (2001) Analysis of point
1038 mutants in the *Caenorhabditis elegans* vesicular acetylcholine transporter reveals domains
1039 involved in substrate translocation. *J Biol Chem* 276:41580-41587.

1040

1041

1042 **FIGURE LEGENDS**

1043

1044 **Figure 1. Alignment of VGLUT protein sequences and the VGLUT3^{A224V/A224V} mouse**
1045 **genomic construct.** (A) Alignment of mouse (mVGLUT3) and human (hVGLUT3) VGLUT3
1046 and mouse (mVGLUT1) VGLUT1 amino acid sequences. The three peptide sequences are
1047 highly conserved (black letters indicate residues conserved in the sequences, and blue
1048 letters indicate residues that are different). The KWAPPLER motif (red boxed text) is
1049 conserved in all three sequences. The mutated alanine residue is in red. This alanine is at
1050 positions 224, 211 and 198 in the mVGLUT3, hVGLUT3 and mVGLUT1 amino acid
1051 sequences, respectively. (B) Schematic representation of the targeting strategy. A targeting
1052 vector was constructed in which the GCG codon (encoding alanine 224) is replaced by a
1053 GTG codon in exon 5. A neomycin resistance selection cassette (flanked by two sites Lox,
1054 LoxP_Neo_LoxP) was integrated downstream of exon 5. An auto-excision of the selection
1055 cassette in a male chimera germ line provided a targeting allele with a valine at position 224
1056 in exon 5 and a LoxP site used for genotyping. (C) Genotyping strategy of mouse VGLUT3
1057 by PCR. Mice were genotyped with two primers (arrowheads P1, P2 in B) flanking each side
1058 of the LoxP site. PCR amplification of the wild-type (WT) allele (+) yielded a 219 bp band,
1059 and the mutated allele (A224V) yielded a 306 bp band in an agarose gel.

1060

1061 **Figure 2. Expression of VGLUT3-p.A211V in cell cultures.** (A) Gel image of RT-PCR
1062 products (negative image) showing no significantly difference between WT and VGLUT3-
1063 p.A211V transcript from BON cells stably expressing each allele. (B-C) Western blot (WB)
1064 quantification of VGLUT3 and VGLUT3-p.A211V in BON cell extracts (B) and in primary
1065 cultures of hippocampal neurons transfected with a VGLUT3 or VGLUT3-p.A211V
1066 expression plasmid (C). VGLUT3-p.A211V expression was reduced by 64% in BON cells (B)
1067 and by 66% in neurons (C). (D, E) Quantification of fluorescence intensity of WT and
1068 VGLUT3-p.A211V in stable BON cells (D) or in synaptic boutons in hippocampal neurons in
1069 culture (E). (F) Western blot detection and quantification of WT and VGLUT1-p.A198V in

1070 BON cell extracts. (G, H) Immunofluorescence microphotographs of VGLUT3 (green) in BON
1071 cells stably transfected with a VGLUT3 (G) or VGLUT3-p.A211V (H) expression plasmid. (I,
1072 J) Hippocampal neurons transiently transfected with a VGLUT3 (I) or VGLUT3-p.A211V (J)
1073 expression plasmid. Nuclei were labeled with DAPI (blue). (K-L) Immunofluorescence of the
1074 WT isoform of VGLUT1 (K, red) or VGLUT1-p.A198V (L, red) in BON cell cultures that were
1075 transiently transfected with expression plasmid. (M-R) Co-localizations of VGLUT3 WT (M,
1076 O, Q, green) or VGLUT3-p.A211V (N, P, R, green) with MAP2 (M, N, red), bassoon (O, P,
1077 red) and PSD95 (Q, R, red) in primary hippocampal neuronal cultures transfected with a
1078 VGLUT3 or VGLUT3-p.A211V plasmid. Areas surrounded by a dashed line are enlarged in
1079 inserts. Scale bar in R: 5 μ m in G-L; 10 μ m in M-R; 1 μ m in insert of M-R.

1080

1081 **Figure 3. Effect of the p.A211V mutation on 3D structure, glutamate vesicular**
1082 **accumulation and release.** (A-H) Three- and two-dimensional model of human VGLUT3 (A-
1083 D) and VGLUT3-p.A211V (E-H) using crystallographic MFS transporter structures as a
1084 template. Packing of the helices viewed from the side (A, C, E, G) or the top (B, F). The
1085 alanine residue (in position 211) of VGLUT3 (A, B) and the valine residue of VGLUT3-
1086 p.A211V (E, F) that are exposed to the pore are shown in pink. Regions boxed in A and E
1087 are enlarged in C and G respectively. (D, H) Close up view and 2-dimensional interactions
1088 diagram of alanine 211 (D) or valine 211 (H). (I) Effect of the p.A211V mutation on H⁺
1089 ionophore carbonyl cyanide m-chlorophenylhydrazone (CCCP) sensitive [³H]L-glutamate
1090 uptake by synaptic vesicles from BON cells stably expressing VGLUT3 (black bars) or
1091 VGLUT3-p.A211V (red bars). The small difference observed between the two populations of
1092 vesicles is not significant (NS). (J-R) Electrophysiological recordings of VGLUT1^{-/-}
1093 hippocampal autaptic neurons infected with lentivirus expressing VGLUT3 (WT) or VGLUT3-
1094 p.A211V isoforms. The number of recorded cells is indicated in bar graphs. Data are pooled
1095 from 2 independent cultures in M and from 4 independent cultures in J, K, L, N, O, P, Q and
1096 R. (J) Top: Representative traces of current responses after two unclamped action potentials
1097 with an interstimulus interval of 25 ms in VGLUT1^{-/-} autaptic neurons (green bars and traces)

1098 expressing VGLUT3 (black bars and traces) or VGLUT3-p.A211V (red bars and traces).
 1099 Artifacts and action potentials are blanked. Bottom: Plot of average EPSC amplitude size
 1100 (first pulse) normalized to WT. (K) Left: Representative traces of current responses after
 1101 application of sucrose (500 mM) for 5 s. Right: Plot of the average readily-releasable pool
 1102 charge normalized to WT. (L) Comparison of the expression levels of WT and VGLUT3-
 1103 p.A211V, determined by measuring immunofluorescence intensities and normalizing to the
 1104 intensities of synaptic marker synaptophysin I (Syp1). (M) Plot of average paired-pulse ratios
 1105 with an interstimulus interval of 25 ms. Data are pooled from 2 independent cultures. (N) Plot
 1106 of average vesicular release probability. Data are pooled from 4 independent cultures. (O)
 1107 Example of mEPSCs traces in autaptic neurons. Scattered points and bar graphs of average:
 1108 mEPSC frequency (P), mEPSC amplitude (Q) and mEPSC charge (R). Data are pooled from
 1109 4 independent cultures.

1110

1111 **Figure 4. Regional expression of VGLUT3, VGLUT3^{A224V/+}, VGLUT3^{A224V/A224V} and**
 1112 **VGLUT3^{A224V/-} in the central nervous system of mice at different ages.** (A-J) Detection
 1113 and quantification of VGLUT3, VGLUT3^{A224V/+}, VGLUT3^{A224V/A224V}, VGLUT3^{A224V/-} mRNA and
 1114 protein expression by *in situ* hybridization or immunohistochemistry on coronal mouse
 1115 brain sections taken at post-natal day 10 (P10, A and B) and the ages of 3 months (C-F), 6
 1116 months (G, H) or 12 months (I, J) in the striatum (Str), hippocampus (Hi), and dorsal and
 1117 median raphe, (DR and MR, respectively). WT, VGLUT3^{A224V/+}, VGLUT3^{A224V/A224V} mice
 1118 expressed a similar level of transcripts (first column, B, D, H, J; Mann-Whitney U test for B, J;
 1119 Kruskal-Wallis test for D, H,; $p > 0.05$, $n = 8$). (B, D, H second column and F) Loss of the
 1120 protein in all areas from P10 until 1 year in VGLUT3^{A224V/A224V} mice ($n = 8$ for each genotype,
 1121 Mann-Whitney U test or Kruskal-Wallis test, * $p < 0.05$, ** $p < 0.01$, *** $p < 0.001$). In
 1122 VGLUT3^{A224V/+} mice, there is a 34% decrease in VGLUT3 in all areas at 3 and 6 months (D,
 1123 H). (E, F) In this experiment, the protein expression of VGLUT3 was compared in WT,
 1124 VGLUT3^{A224V/A224V} and VGLUT3^{A224V/-} mice ($n = 8$) in the striatum, hippocampus and dorsal
 1125 raphe. VGLUT3 expression decreased by 70% in VGLUT3^{A224V/A224V} mice and further

1126 decreased by 84% in VGLUT3^{A224V/-} mice in the striatum (Kruskal-Wallis test; in the striatum,
 1127 WT vs VGLUT3^{A224V/+}, $p = 0.0043$; WT vs VGLUT3^{A224V/A224V}, $p = 0.0043$; WT vs
 1128 VGLUT3^{A224V/-}, $p = 0.0012$. In the hippocampus, WT vs VGLUT3^{A224V/+}, $p = 0.01$; WT vs
 1129 VGLUT3^{A224V/A224V}, $p = 0.0043$; WT vs VGLUT3^{A224V/-}, $p = 0.0012$. In raphe nuclei, WT vs
 1130 VGLUT3^{A224V/+}, $p = 0.0571$; WT vs VGLUT3^{A224V/A224V}, $p = 0.0159$; WT vs VGLUT3^{A224V/-}, $p =$
 1131 0.0286). (K, L) Western blot detection (K) and quantification (L) of VGLUT3 in the cortex
 1132 (Cx), striatum (Str) and hippocampus (Hi) of VGLUT3^{A224V/+} and VGLUT3^{A224V/A224V} mice at 3
 1133 months ($n = 5$; Kruskal-Wallis test; ** $p < 0.01$).

1134

1135 **Figure 5. Expression of VGLUT3-p.A224V in soma and terminals of VGLUT3-positive**
 1136 **neurons in the brain of WT and VGLUT3^{A224V/A224V} mice.** (A-H) Immunofluorescence
 1137 visualization and quantification of VGLUT3 in the striatum (A, C) and in the CA1 pyramidal
 1138 field of the hippocampus (E, G) in WT (A, E) and VGLUT3^{A224V/A224V} mice (C, G). VGLUT3
 1139 expression is substantially reduced in terminals of the striatum (B, -69%) and hippocampus
 1140 (F, -72%), whereas its expression is unchanged in the soma of TANs and basket cells (D, H).
 1141 (I-J) Electron microphotographs of the soma of TANs in striatal sections of WT (I) and
 1142 VGLUT3^{A224V/A224V} (J) mice. VGLUT3 is labeled with gold particles. The distribution of
 1143 VGLUT3 labeling is similar in WT (I) and VGLUT3^{A224V/A224V} (J) mice. Abbreviations: er,
 1144 endoplasmic reticulum; n, nucleus; or, stratum oriens of the hippocampus; py, stratum
 1145 pyramidale of the hippocampus; rad, Stratum radiatum. Scale bar: 35 μm in A, C, E, G; 1 μm
 1146 in I, J.

1147

1148 **Figure 6. The p.A211V mutation does not alter VGLUT3 mobility.** (A) Representative
 1149 image sequence depicting the initial fluorescence in the chosen boutons (white arrow), the
 1150 loss of fluorescence after bleaching (time point 02:10 min), and the gradual recovery of
 1151 fluorescent material in the bleached region in hippocampal cultures expressing either
 1152 VGLUT3-venus or VGLUT3-p.A211V-venus. (B) Kinetics of FRAP over 75 minutes in

1153 neurons expressing VGLUT3-venus or VGLUT3-p.A211V-venus. Average recovery curves
1154 (error bars represent SEM) are shown in black for VGLUT3-venus and in red for VGLUT3-
1155 p.A211V-venus. Inset at top shows FRAP curves during the first 10 min, with images taken
1156 every 5 seconds. (C) Amplitude of recovery for VGLUT3-venus or VGLUT3-p.A211V-venus
1157 in bleached boutons 60 minutes after recovery from bleaching. Data are pooled from 5
1158 independent cultures for FRAP and 3 independent cultures for Fast FRAP (n = 25 boutons
1159 per condition).

1160

1161 **Figure 7. Behavioral analysis of VGLUT3^{A224V/A224V} mice.** (A) In the open field, WT
1162 littermates, VGLUT3^{A224V/+} and VGLUT3^{A224V/A224V} mice spent the same time at the center of
1163 the open field (Kruskal-Wallis test, $p > 0.05$) and presented the same locomotor activity at
1164 the center and the periphery of the open field (Kruskal-Wallis test, $p > 0.05$). The number of
1165 animals is indicated in the bar graph. (B) Anxiety levels assessed in the elevated plus maze
1166 were similar in WT, VGLUT3^{A224V/+} and VGLUT3^{A224V/A224V} mice (Kruskal-Wallis test, $p > 0.05$).
1167 Horizontal exploration was measured for 6 min. No difference was found in total entries or in
1168 the time spent in open arms between the WT and the VGLUT3 mutant mice (Kruskal-Wallis
1169 test, $p > 0.05$). (C) Spontaneous locomotor activity of naive WT, VGLUT3^{A224V/+} and
1170 VGLUT3^{A224V/A224V} mice. Horizontal locomotor activity was recorded for five hours (first hour
1171 during the light cycle followed by four hours during the dark cycle). Spontaneous locomotor
1172 activity was similar in WT and mutant animals (Kruskal-Wallis test, $p > 0.05$). (D) Left: Time
1173 course of the locomotor effect of cocaine (10 mg/kg, ip) in WT (n = 7) and VGLUT3^{A224V/A224V}
1174 (n = 6) mice. Animals were placed in the cyclotron for 240 min for habituation and then
1175 injected with saline (NaCl 0.9%), placed back in the cyclotron for 60 min and then injected
1176 with cocaine (10 mg/kg). Following cocaine injection, locomotion was recorded for 95 min.
1177 There was no significant difference in locomotor activity between WT and mutant mice that
1178 were treated with cocaine (repeated-measures ANOVA, $p > 0.05$). Right: Cumulative
1179 horizontal locomotor activity over 60 min for saline (Sal)-treated or 95 min for cocaine-
1180 injected (Coc) WT (n = 7) and VGLUT3^{A224V/A224V} mice (n = 6). No difference was observed in

1181 cumulative locomotor activity following saline or cocaine injection between the WT and the
1182 VGLUT3^{A224V/A224V} mice (Mann-Whitney U test, $p > 0.05$).
1183 (E-H) Behavioral analysis of mice expressing only one copy of VGLUT3-pA224V
1184 (VGLUT3^{A224V/-}). (E) In the open field, WT and VGLUT3^{A224V/-} mice spent the same time in
1185 the center area and crossed the periphery or the central area the same number of times
1186 (Mann-Whitney U test, $p > 0.05$). (F) WT and VGLUT3^{A224V/-} mice presented the same
1187 anxiety level when assessed in the elevated plus maze (Mann Whitney U test, $p > 0.05$). (G)
1188 Time course of the locomotor effect of cocaine (10 mg/kg, ip) in WT mice and VGLUT3^{A224V/-}
1189 mice. Animals were placed in the cyclotron as described in (D). No significant differences in
1190 locomotor activity were observed after cocaine injection between the WT and the mutant
1191 mice (repeated-measures ANOVA, $p > 0.05$). (H) Cumulative horizontal locomotor activity
1192 during the first 120 min in the cyclotron or 60 min after saline injection (Sal) and 95 min after
1193 cocaine injection (Coc, 10 mg per Kg i.p) in WT (n = 16) and VGLUT3^{A224V/-} mice (n = 15).
1194 During the first two hours in the cyclotron, the locomotor activity of the VGLUT3^{A224V/-} mice
1195 was higher than the locomotor activity of the WT mice (Mann-Whitney U test, $p = 0.0329$).
1196 After saline injection, the VGLUT3^{A224V/-} mice were slightly hyperactive compared with the
1197 WT mice (Mann-Whitney U test, $p = 0.0270$). No difference was observed in cumulative
1198 locomotor activity following cocaine injection between the WT and the VGLUT3^{A224V/-} mice
1199 (Mann-Whitney U test, $p = 0.1725$).

1200

1201 **Figure 8. The p.A224V mutation does not influence VGLUT3-dependent vesicular**
1202 **synergy.** [³H]5-HT reserpine-sensitive uptake in cortical synaptic vesicles was measured in
1203 the presence (+) or absence (-) of L-glutamate (Glut). [³H]5-HT reserpine-sensitive vesicular
1204 accumulation was augmented by L-glutamate (10 mM) in the cortical synaptic vesicles of WT
1205 (+27%), VGLUT3^{A224V/+} (+27%), VGLUT3^{A224V/A224V} (+22%) and VGLUT3^{A224V/-} mice (+22%)
1206 but not in VGLUT3^{-/-} mice due to the absence of VGLUT3 from synaptic vesicles.

1207

1208 **Figure 9. High-resolution fluorescence imaging by STED revealed a decrease in**
 1209 **VGLUT3-positive vesicles in mutant mice.** (A-E) Co-detection by STED microscopy of
 1210 VGLUT3 (red) and synaptophysin (green) in axonal varicosities of the striatum of WT (A),
 1211 VGLUT3^{A224V/+} (B), VGLUT3^{A224V/A224V} (C), VGLUT3^{A224V/-} (D) and VGLUT3^{-/-} (E) mice.
 1212 VGLUT3 and Synaptophysin immunofluorescence events were observed as round shaped
 1213 elements within striatal varicosities of WT, VGLUT3^{A224V/+}, VGLUT3^{A224V/A224V} and
 1214 VGLUT3^{A224V/-} mice. In VGLUT3^{-/-} mice, only synaptophysin was detected. Note the
 1215 decrease in the number of VGLUT3 immunopositive puncta in VGLUT3^{A224V/+},
 1216 VGLUT3^{A224V/A224V} and VGLUT3^{A224V/-} mice compared with WT mice. (F) Quantification of
 1217 VGLUT3 and synaptophysin immunofluorescent events per varicosities. The numbers of
 1218 VGLUT3 immunopositive puncta were quantified in striatal axonal varicosities of WT,
 1219 VGLUT3^{A224V/+}, VGLUT3^{A224V/A224V}, VGLUT3^{A224V/-} and VGLUT3^{-/-} mice after double
 1220 immunofluorescence (80, 76, 76, 90 and 105 varicosities per animal were quantified in 6 WT,
 1221 6 VGLUT3^{A224V/+}, 6 VGLUT3^{A224V/A224V}, 6 VGLUT3^{A224V/-} and 5 VGLUT3^{-/-} mice, respectively).
 1222 Note that the number of VGLUT3 puncta decreased with the genotype. (G) Correlation
 1223 between number of VGLUT3-positive puncta determined by STED and VGLUT3 expression
 1224 determined by immunohistochemistry. The correlation was statistically significant (linear
 1225 regression, $r^2 = 0.9528$; $p = 0.0044$). (H) Effect of laser power on the number of events of
 1226 VGLUT3-fluorescence detection. The blue arrows indicate the laser power that was selected for
 1227 the images shown in A-E. The number of puncta per varicosity did not differ significantly when
 1228 the laser power increased (Kruskal-Wallis test, $p > 0.05$). Scale bar in E: 500 nm in A-E.

1229

1230 **Figure 10. Putative models depicting the reduction in VGLUT3 at the synapses of**
 1231 **different mouse genotypes.** In this report, we investigated mouse models with variable
 1232 levels of VGLUT3 expression: WT mice (two copies of WT VGLUT3 isoform; 100%),
 1233 heterozygous mice (one copy of WT VGLUT3 isoform and one copy of VGLUT3-p.A224V
 1234 allele; 67%), homozygous mice (two copies of the mutated VGLUT3-p.A224V allele; 28%),
 1235 VGLUT3^{A224V/-} mice (expressing only one copy of the mutated VGLUT3-p.A224V allele; 21%),

1236 and VGLUT3 knockout mice (no copy of VGLUT3; 0%). (A) The black curve shows the
1237 relationship between VGLUT3 expression (detected by immunautoradiography) and the
1238 activity of VGLUT3 (indirectly assessed by measuring vesicular synergy). VGLUT3 activity
1239 did not decline in proportion to the amount of VGLUT3 in the expression range between
1240 100% and 21% (black curve). The absence of a correlation between these two sets of
1241 measurements explains the virtual lack of a VGLUT3-dependent phenotype in our panel of
1242 mutants. This model predicts that these phenotypes will be observed in the gray zone of the
1243 curve (red curve).

1244 (B) Three putative models that may account for the reduction in VGLUT3 at the synapses are
1245 compared with our experimental results. In WT mice, numerous copies of VGLUT3 are
1246 uniformly distributed between synaptic vesicles, and these vesicles are “normally” loaded
1247 (100% gray level) with glutamate. In model 1 (molecular model), VGLUT3 copies are
1248 uniformly decreased in all vesicles of VGLUT3^{A224V/A224V} mice. In this model, the vesicular
1249 content of glutamate is minimally decreased in all vesicles. This decrease in glutamatergic
1250 quantal size cannot be observed with bulk methods, such as vesicular uptake or behavioral
1251 measurements, but can be detected by more sensitive electrophysiological techniques.
1252 Model 1 would be compatible with i) an absence of change in vesicular uptake (observed in
1253 BON cells) and vesicular synergy (VS, observed in cortical vesicles) and ii) a decrease in the
1254 amplitudes of the mEPSCs that were observed in recordings of isolated neurons. Model 2
1255 (vesicular model) is based on the STED high-resolution inspection of VGLUT3-positive
1256 terminals in our panel of mutants. In this model, in a small proportion of vesicles, the number
1257 of VGLUT3-p.A224V copies per vesicles is similar (or minimally decreased) to that found in
1258 WT neurons. According to the electrophysiological recordings of autapses, these vesicles
1259 may contain normal levels of glutamate and be preferentially docked. The remaining vesicles
1260 (80%) will contain neither VGLUT3 nor glutamate. This model is consistent with the
1261 decreased frequency of the mEPSCs.

1262 A mixed model (model 3) of these two models may better explain all of our experimental
1263 results. In this model, we found vesicles without VGLUT3, a small proportion of vesicles

1264 expressing the correct number of VGLUT3-p.A224V copies and a third population of vesicles
1265 in which the number of VGLUT3 copies were uniformly decreased in all vesicles of the
1266 synapses from VGLUT3^{A224V/A224V} mice.
1267

1268 **Table I. List of mutants mice used in the study**

	Number of copies of VGLUT3 allele	VGLUT3 ⁺	VGLUT3 ^{A224V}	VGLUT3 ⁻
Name				
WT or VGLUT3^{+/+}		2	0	0
VGLUT3^{A224V/+}		1	1	0
VGLUT3^{A224V/A224V}		0	2	0
VGLUT3^{A224V/-}		0	1	1
VGLUT3^{-/-}		0	0	2

1269

1270

1271 **Table II. Percentage of decrease in VGLUT3 expression as determined by**
 1272 **immunoautoradiography in the striatum, hippocampus and raphe nuclei of**
 1273 **VGLUT3^{A224V/+}, VGLUT3^{A224V/A224V} and VGLUT3^{A224V/-} at 10 days postnatal (P10) and 3, 6**
 1274 **or 12 months of age (mo).**

		Age	P10	3 mo	6 mo	12 mo
Brain area	Genotype	% VGLUT3 decrease				
Striatum	VGLUT3 ^{A224V/+}	N.A.	34	50	N.A.	
	VGLUT3 ^{A224V/A224V}	83	76	77	85	
	VGLUT3 ^{A224V/-}	N.A.	84	N.A.	N.A.	
Hippocampus	VGLUT3 ^{A224V/+}	N.A.	26	38	N.A.	
	VGLUT3 ^{A224V/A224V}	76	69	70	78	
	VGLUT3 ^{A224V/-}	N.A.	88	N.A.	N.A.	
Dorsal Raphe	VGLUT3 ^{A224V/+}	N.A.	16	24	N.A.	
	VGLUT3 ^{A224V/A224V}	50	46	61	77	
	VGLUT3 ^{A224V/-}	N.A.	71	N.A.	N.A.	
Median Raphe	VGLUT3 ^{A224V/+}	N.A.	20	29	N.A.	
	VGLUT3 ^{A224V/A224V}	N.A.	74	63	N.A.	

1275

1276

1277 **Table III. Percentage decrease in VGLUT3 expression as determined by western blot**
 1278 **analysis of the cortex, striatum and hippocampus of heterozygous and homozygous**
 1279 **VGLUT3-p.A224V expressing mice at 3 months of age (mo).**

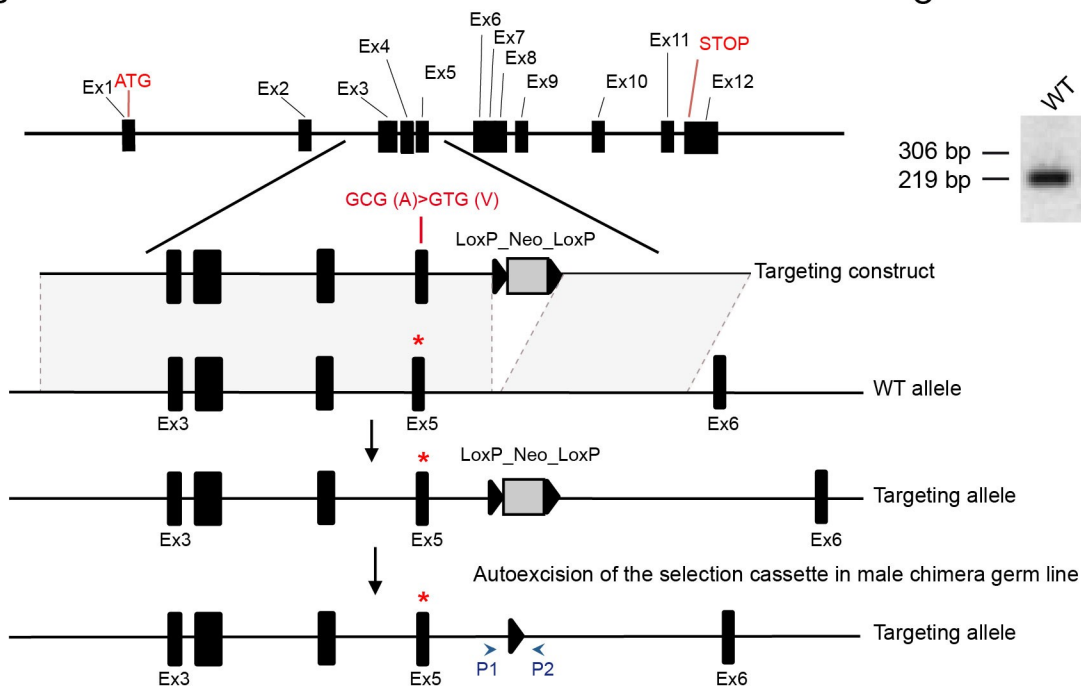
	Age 3 mo	
Brain area	Genotype	% VGLUT3 decrease
Cortex	VGLUT3 ^{A224V/+}	63
	VGLUT3 ^{A224V/A224V}	72
Striatum	VGLUT3 ^{A224V/+}	55
	VGLUT3 ^{A224V/A224V}	85
Hippocampus	VGLUT3 ^{A224V/+}	47
	VGLUT3 ^{A224V/A224V}	70

1280
1281

A

mVGLUT3 STLNMFIPSAARVHYGCVMGVRIQLQGLVEGVITYPACHGMW**SKWAPPLERS**RLATT**S**FCGS 240
hVGLUT3 STLNMFIPSAARVHYGCVMCVRIQLQGLVEGVITYPACHGMW**SKWAPPLERS**RLATT**S**FCGS 227
mVGLUT1 STLNMLIPSAARVHYGCVIFVRIQLQGLVEGVITYPACHGIW**SKWAPPLERS**RLATT**A**FCGS 214

B



C

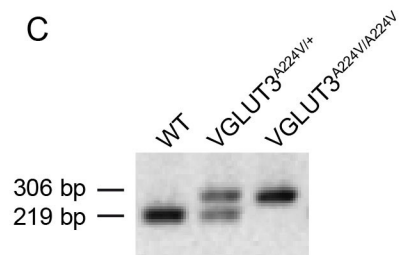


Figure 1 Ramet et al.

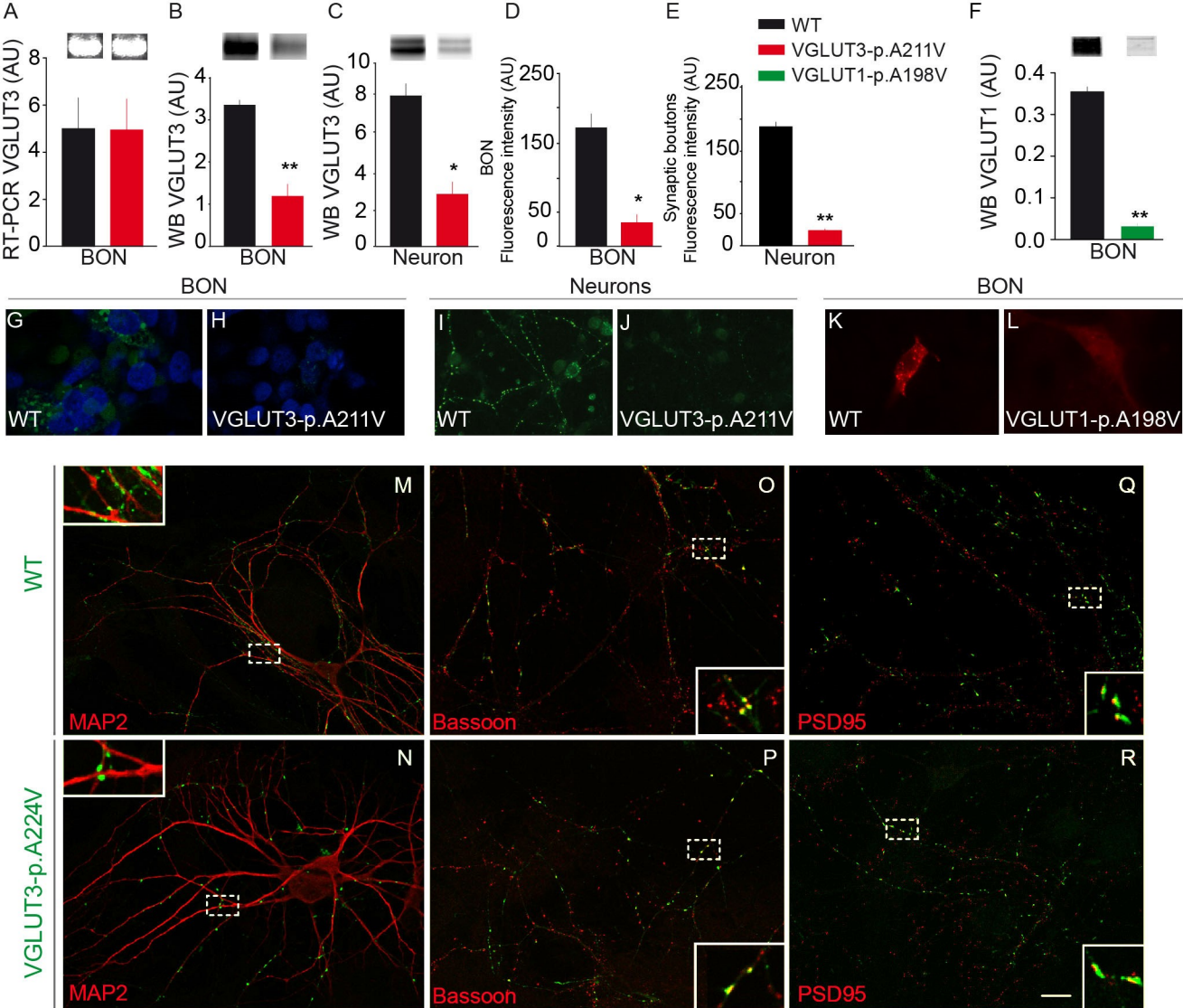


Figure 2 Ramet et al.

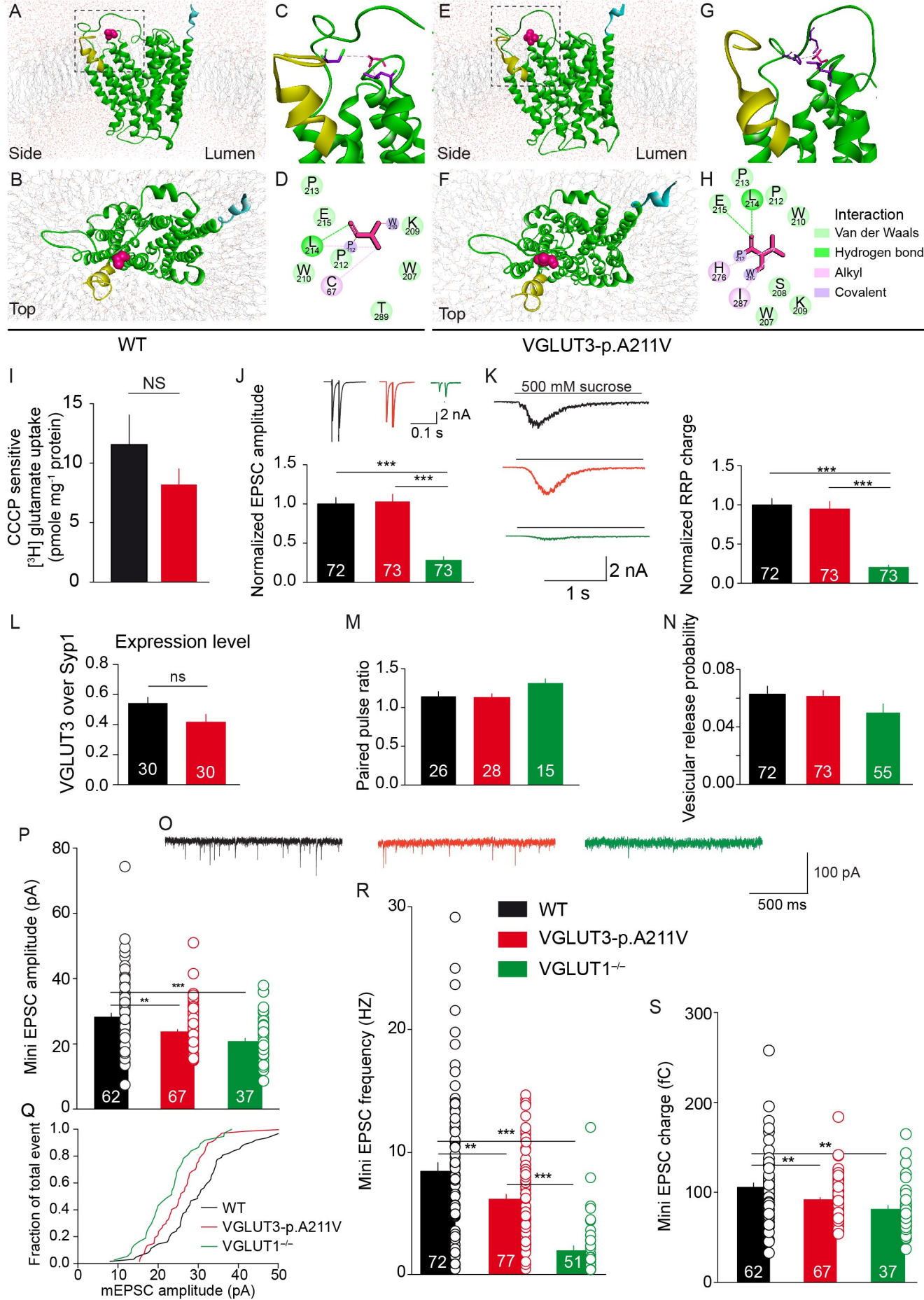


Figure 3 Ramet et al.

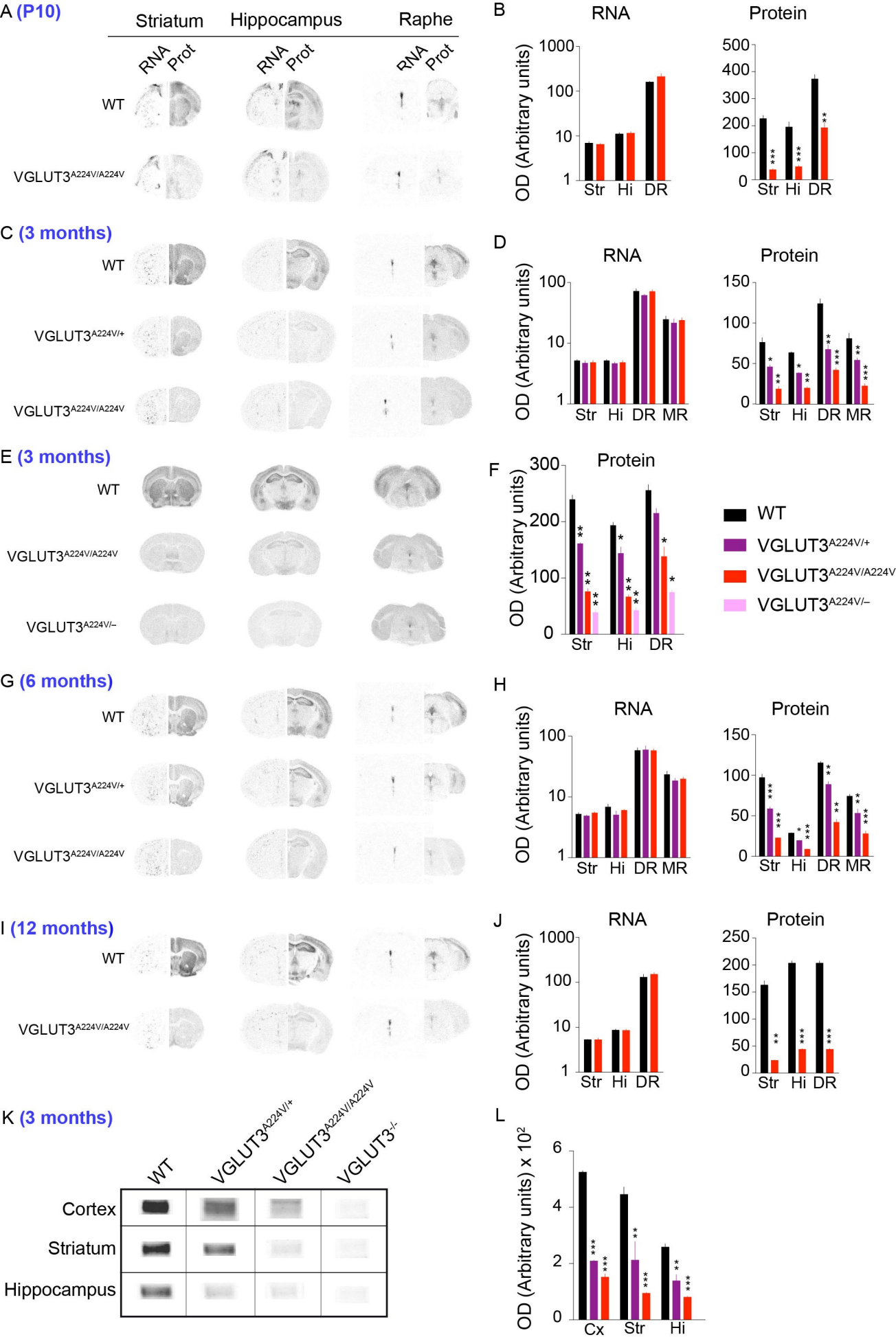


Figure 4 Ramet et al.

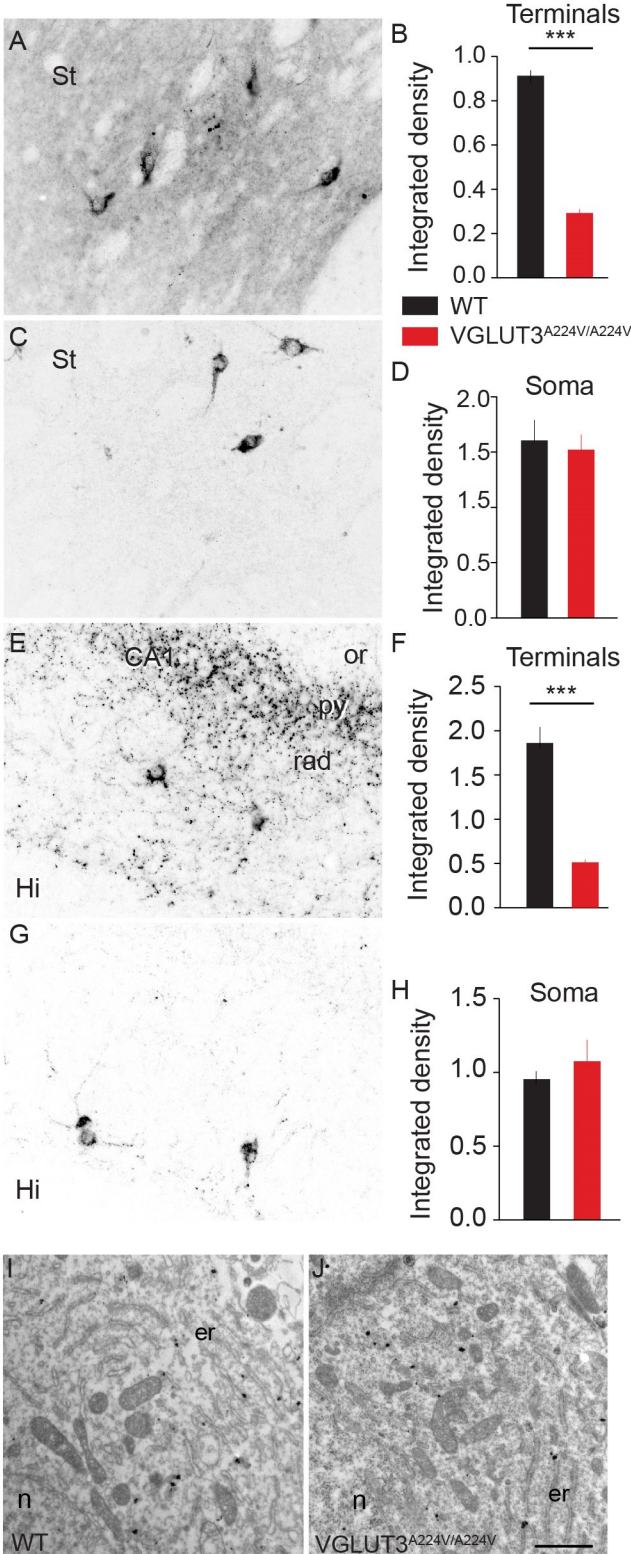


Figure 5 Ramet et al.

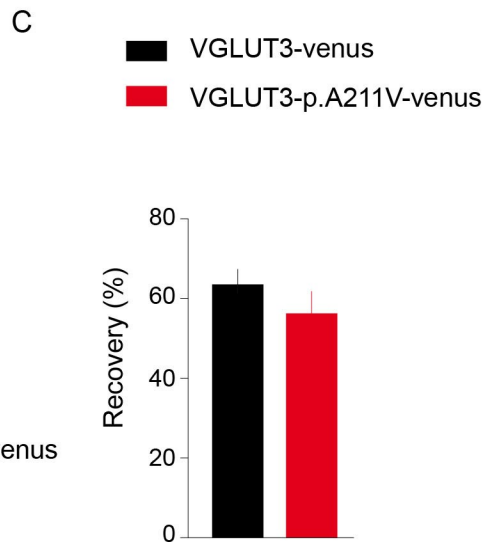
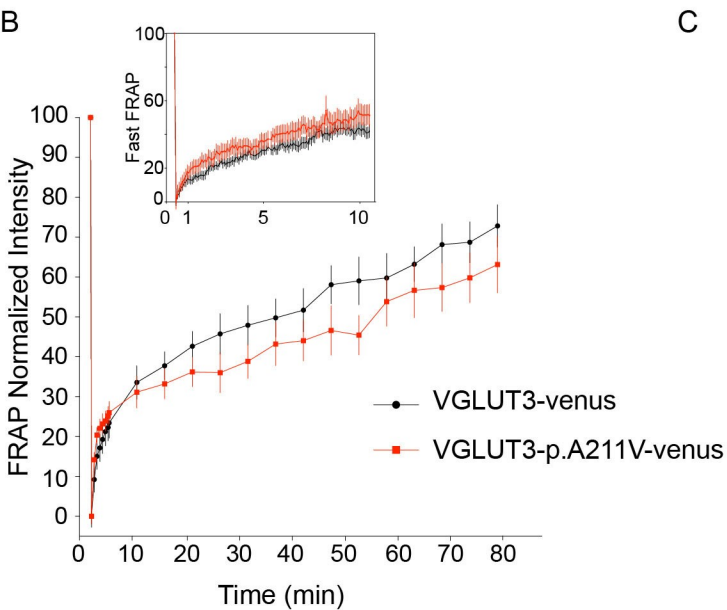
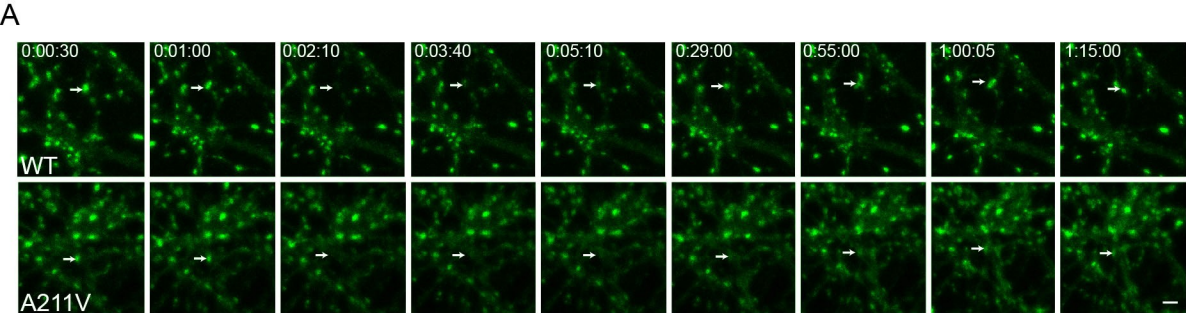
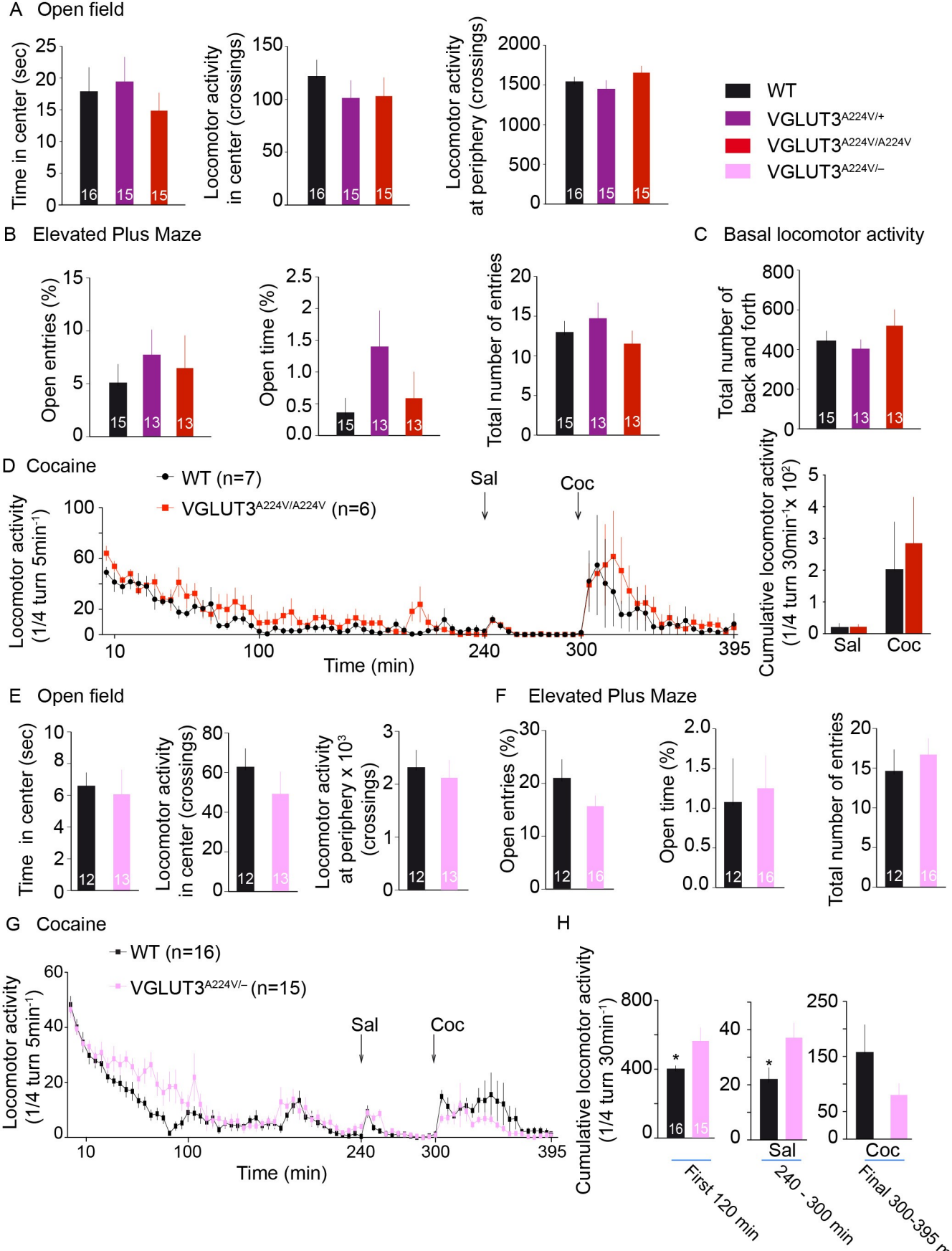


Figure 6 Ramet et al.



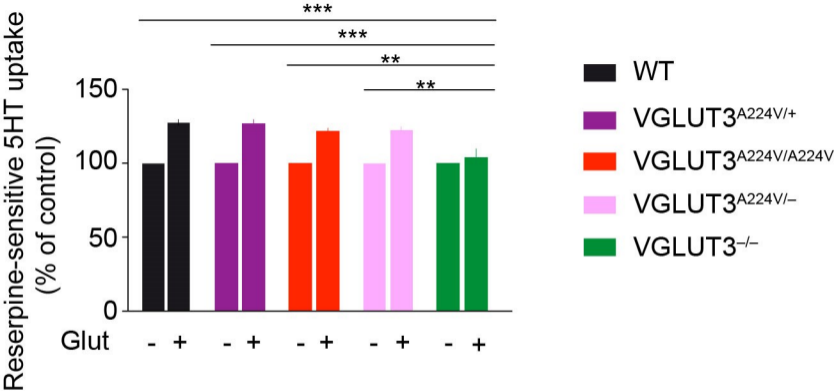


Figure 8 Ramet et al.

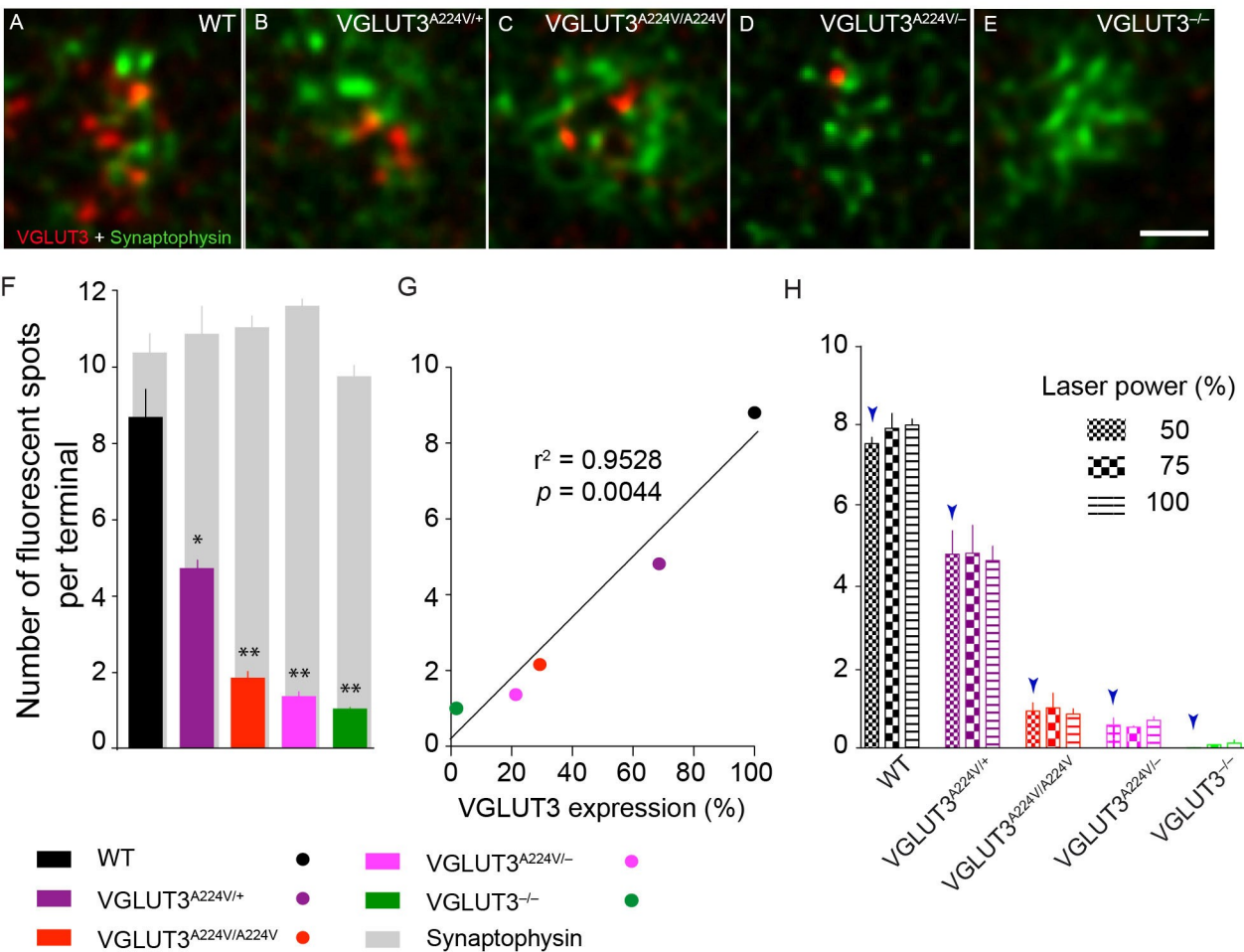


Figure 9 Ramet et al.

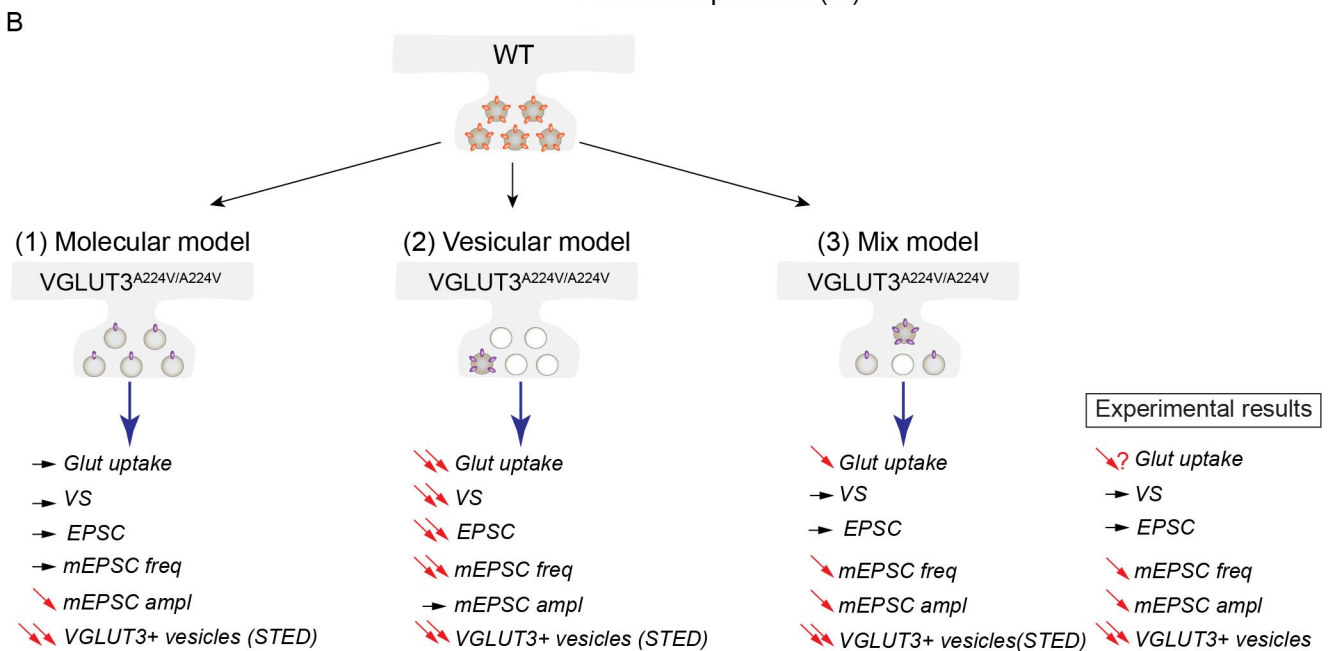
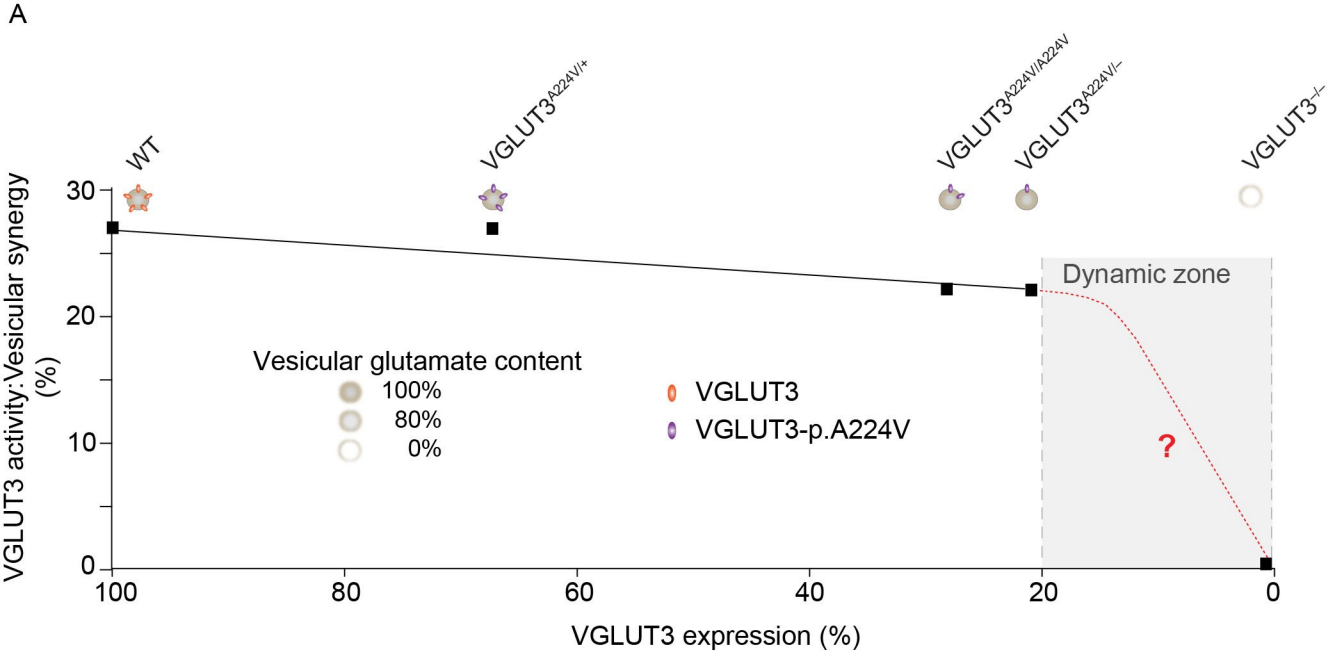


Figure 10 Ramet et al.